Global Change Biology (2006) **12**, 1107–1138, doi: 10.1111/j.1365-2486.2006.01120.x

# The regional variation of aboveground live biomass in old-growth Amazonian forests

YADVINDER MALHI*†, DANIEL WOOD†, TIMOTHY R. BAKER§, JAMES WRIGHT¶, OLIVER L. PHILLIPS§, THOMAS COCHRANE‖, PATRICK MEIR†, JEROME CHAVE**, SAMUEL ALMEIDA††, LUZMILLA ARROYO‡‡, NIRO HIGUCHI§§, TIMOTHY J. KILLEEN¶¶, SUSAN G. LAURANCE‖‖, WILLIAM F. LAURANCE‖‖, SIMON L. LEWIS§, ABEL MONTEAGUDO***†††, DAVID A. NEILL‡‡‡, PERCY NÚÑEZ VARGAS§§§, NIGEL C. A. PITMAN¶¶¶, CARLOS ALBERTO QUESADA§, RAFAEL SALOMÃO††, JOSÉ NATALINO M. SILVA‖‖‖****, ARMANDO TORRES LEZAMA††††, JOHN TERBORGH¶¶¶, RODOLFO VÁSQUEZ MARTÍNEZ†††and BARBARA VINCETI‡‡‡‡

**Oxford University Centre for the Environment, South Parks Road, Oxford, UK, †School of GeoSciences, University of Edinburgh, Darwin Building, Mayfield Road, Edinburgh, UK, §Earth and Biosphere Institute, Geography, University of Leeds, Leeds, UK, ¶Department of Geography, University of Southampton, Southampton, UK, ‖Agteca, Casilla Postal 6329, Santa Cruz, Bolivia, **Laboratoire Evolution et Diversité Biologique, CNRS/UPS, Toulouse, France, ††Museu Paraense Emilio Goeldi, Belém, Brazil, ‡‡Museo Noel Kempff Mercado, Santa Cruz, Bolivia, §§Instituto National de Pesquisas Amazônicas, Manaus, Brazil, ¶¶Center for Applied Biodiversity Science, Conservation International, Washington, DC, USA, ‖‖Smithsonian Tropical Research Institute, Balboa, Panama, ***Herbario Vargas, Universidad Nacional San Antonio Abad del Cusco, Cusco, Peru, †††Proyecto Flora del Perú, Jardin Botanico de Missouri, Oxapampa, Perú, ‡‡‡Fundacion Jatun Sacha, Quito, Ecuador, §§§Herbario Vargas, Universidad Nacional San Antonio Abad del Cusco, Cusco, Peru, ¶¶¶Center for Tropical Conservation, Duke University, Durham, NC, USA, ‖‖‖CIFOR, Tapajos, Brazil, ****EMBRAPA Amazonia Oriental, Belém, Brazil, ††††INDEFOR, Facultad de Ciencias Forestales y Ambientale, Universidad de Los Andes, Mérida, Venezuela, ‡‡‡‡International Plant Genetic Resources Institute, Rome, Italy*

**Abstract**

**The biomass of tropical forests plays an important role in the global carbon cycle, both as a dynamic reservoir of carbon, and as a source of carbon dioxide to the atmosphere in areas undergoing deforestation. However, the absolute magnitude and environmental determinants of tropical forest biomass are still poorly understood. Here, we present a new synthesis and interpolation of the basal area and aboveground live biomass of old-growth lowland tropical forests across South America, based on data from 227 forest plots, many previously unpublished. Forest biomass was analyzed in terms of two uncorrelated factors: basal area and mean wood density. Basal area is strongly affected by local landscape factors, but is relatively invariant at regional scale in moist tropical forests, and declines significantly at the dry periphery of the forest zone. Mean wood density is inversely correlated with forest dynamics, being lower in the dynamic forests of western Amazonia and high in the slow-growing forests of eastern Amazonia. The combination of these two factors results in biomass being highest in the moderately seasonal, slow growing forests of central Amazonia and the Guyanas (up to 350 Mg dry weight ha$^{-1}$) and declining to 200–250 Mg dry weight ha$^{-1}$ at the western, southern and eastern margins. Overall, we estimate the total aboveground live biomass of intact Amazonian rainforests (area 5.76 $\times$ 10$^6$ km$^2$ in 2000) to be 93 $\pm$ 23 Pg C, taking into account lianas and small trees. Including dead biomass and belowground biomass would increase this value by approximately 10% and 21%, respectively, but the spatial variation of these additional terms still needs to be quantified.**

*Keywords:* Amazonia, biomass, carbon, soil fertility, tropical forests, wood density

*Received 10 January 2005; revised version received 18 August 2005; accepted 3 October 2005*

Correspondence: Y. Malhi, Oxford University Centre for the Environment, South Parks Road, Oxford OX1 3QY, UK, tel: + 44 (0)1865 285188, fax + 44 (0)1865 271929, e-mail: ymalhi@ouce.ox.ac.uk

## Introduction

The lowland tropical forests of South America account for about half of the world's tropical forest area (FAO, 2001). They are estimated to account for 30% of global productivity (Roy *et al*., 2001) and 25% of global biodiversity (Groombridge & Jenkins, 2003). They are also being cleared at rapid rates (Achard *et al*., 2002), and are, thus, a major carbon source, equivalent to 5–10% of fossil fuel emissions in the 1990s (Achard *et al*., 2004). Quantifying the amount of carbon stored and cycled in these forests is clearly important. In addition, there is accumulating evidence that old-growth tropical forests may be accelerating in growth (Lewis *et al*., 2004), recruitment and mortality (Phillips & Gentry, 1994; Phillips *et al*., 2004), increasing in biomass (Malhi & Grace, 2000; Baker *et al*., 2004a) and shifting in ecological composition (Phillips *et al*., 2002; Laurance *et al*., 2004), but there is little understanding on the constraints and determinants of current forest biomass.

The absolute magnitude and spatial variation of biomass in these forests are poorly quantified. Recent estimates of forest biomass have come from either interpolation of plot studies (Houghton *et al*., 2001), or are based on a combination of modelling and remote-sensing approaches (Houghton *et al*., 2001; Potter *et al*., 2001). Interpolation from site studies is hampered by the low number of systematically consistent compilations, or by only partial inventories of large trees or partial geographical coverage, such as RADAMBRASIL (Brown & Lugo, 1992; Fearnside, 1997). Model studies, on the other hand, are based on predictions of productivity, and often incorporate untested assumptions about the relationship between gross photosynthesis, wood productivity and total biomass (Malhi *et al*., in preparation).

Here, we present a data synthesis and interpolation of results based on a compilation of biomass and basal area data across the South American lowland tropical forests. Many of these site data are previously unpublished, and/or are part of the RAINFOR network (Malhi *et al*., 2002) of Neotropical forest plots; other data are gathered from published or grey literature. We incorporate data from 226 sites in eight South American countries, to our knowledge the most spatially extensive dataset to date on neotropical forest biomass. We also include data from one well-studied central American site (Barro Colorado Island, Panama) in the analysis, but not in the spatial interpolations.

A novel feature that is accounted for in this analysis is biogeographic variation in mean forest wood density that is driven by shifts in tree species composition (Terborgh & Andresen, 1998). Analysing a subset of the plots presented here (Baker *et al*., 2004b) found that spatial variations in wood density play a major role in determining spatial variations in biomass. The mean wood density was found to be inversely correlated with wood productivity, with more dynamic forests having more light wood species. Moreover, aboveground wood productivity appears related to soil properties, but not to climate (Malhi *et al*., 2004). Our aim here is to assess how this variation in wood density affects regional patterns and total estimates of Amazonian forest biomass.

For the study here, we focus on South American tropical lowland forests. Ninety-five percent of these forests lie in a contiguous block in the Amazon and Orinoco basins and Guyana shield and are floristically interconnected; for convenient shorthand these will be referred to as 'Amazonian forests'. The remaining 5% lie in small blocks west of the Andes, and in fragments in eastern Brazil and on the Atlantic coast. We focus solely on extrapolation of biomass from apparently undisturbed old-growth forests. Hence, our extrapolated maps are estimates of the undisturbed biomass of Amazonian forests, and we do not try to account for human impacts such as forest degradation, cryptic forest impoverishment, which may be occurring at rates of 10–15 000 $km^2 a^{-1}$, and edge effects (Laurance *et al*., 1997; Nepstad *et al*., 1999). Our aim is to understand how the background biomass of these forests varies with regional-scale environmental factors, not to quantify human impacts on these forests.

## Materials and methods

### *Field sites, forest cover and climate*

The data used in this study are listed in Table A1 in Appendix A, and mapped in Fig. 1. The dataset is a compilation of published values and unpublished data compiled by the authors within the RAINFOR project (Malhi *et al*., 2002, www.geog.leeds.ac.uk/projects/rainfor), with the source indicated in Table 1. In total, there are 227 plots in the dataset, with reasonable distribution across Amazonia. The largest spatial gaps in our dataset are Colombia and the southern Brazilian Amazon. For the majority of sites (open circles in Fig. 1) only data on basal area were available (in general from published data). For a subset of sites (filled circles; bold type in the 'biomass' column in Table A1) the aboveground dry weight live biomass (henceforth 'AGL biomass') was directly estimated within the RAINFOR project, using individual tree diameter data and taxonomy to directly account for wood density and the size-class distribution of stems (Baker *et al*., 2004b). Only trees with diameter at 1.3 m (dbh) > 10 cm were


**Fig. 1** Forest site locations where basal area measurements have been taken in lowland South American tropical forests. Filled circles indicate sites where the availability of taxonomic data permitted direct calculation of mean wood density; open circles indicate sites where only information on total basal area was available.

**Table 1** Cross-correlation matrix of forest plot basal area against various climatic variables, including the multi-variate ENSO index

| | Basal area | Mean dry season length | Mean monthly rainfall | Mean monthly temperature | Mean monthly solar | ENSO index |
|---|---|---|---|---|---|---|
| Basal area | 1 | | | | | |
| Mean dry season length | −0.25 **(−0.38)** | 1 | | | | |
| Mean monthly rainfall | 0.28 **(0.38)** | −0.88 **(−0.88)** | 1 | | | |
| Mean monthly temperature | −0.01 **(−0.01)** | −0.02 **(0.05)** | −0.16 **(−0.23)** | 1 | | |
| Mean monthly solar | −0.08 **(−0.22)** | 0.50 **(0.48)** | −0.30 **(−0.28)** | −0.49 **(−0.47)** | 1 | |
| ENSO index | −0.21 **(−0.16)** | 0.22 **(0.36)** | −0.23 **(−0.24)** | −0.46 **(0.05)** | 0.51 **(0.17)** | 1 |

Figures in normal type are for all forest plot data; figures in bold type in brackets are after removal of 28 outlier plots as described in the text.
ENSO, El Nino-southern oscillation.

considered in plot-level estimates of biomass; small trees and lianas may account for up to a further 10% of biomass (Phillips *et al*., 1998; DeWalt & Chave, 2004). Biomass for these plots was estimated using individual tree allometric relationships derived from direct sampling in central Amazonia, with additional incorporation of wood density data for each species; details are given in Baker *et al*. (2004b).

The approach to estimate biomass applied here tries to take into account spatial variation in basal area, stem size distribution and wood density. One factor that is still not accounted for is spatial variation in allometry (i.e. the tree height and biomass supported for a given tree basal area). The data that exist to date (T. Baker, unpublished data) give no indication of a clear relationship between allometry and environmental factors, although it would be expected from hydrological considerations (Meinzer *et al*., 1999; 2001) that tree height per unit basal area would reduce with increasing dry season length. As the biomass estimates derived here apply an allometric relationship derived for the central Amazon near Manaus, it is likely that tree height and biomass at the dry margins of Amazonia will be overestimated.

We concentrate our analyses and extrapolations on the continuous lowland tropical rainforest region centred on the Amazon Basin. The dry limits of 'rainforests' are rather arbitrary and vary according to source and climatic dataset applied. Here, we use a definition of a lowland tropical rainforest as equivalent to the 'rainforest' plus 'tropical moist forest' categories in the FAO Global Forest Resources Assessment 2000 (FAO Forestry Paper 140, data available online at http://www.fao.org/forestry/fo/fra), and at an elevation less than 1000 m. The FAO defines tropical forests as forests with mean temperature in all months over 18 °C, with 0–3 dry months (rainforests) or 3–5 dry months (moist deciduous forest), where dry months are defined as months where total precipitation in millimeters is equal to or less than twice the mean temperature in degree Celsius.[1] Some estimates of tropical forest area also include the 'tropical dry forest category'. However, this category frequently grades into woody savanna regions, and is excluded from the current analysis. The forest cover map was coarsened to 0.5° resolution to be compatible with the climate dataset. Our study area included significant areas outside the Amazon watershed, in particular large areas of the Orinoco Basin, the Guyana lowlands and the Brazilian periphery east of the mouth of the Amazon. However, these areas form a phytogeographic continuum with Amazon lowland rainforest, and hence, it is reasonable to adopt the shorthand 'Amazonia' to describe this entire lowland tropical forest region. Other recent maps of forest cover (Achard *et al*., 2002; DeFries *et al*., 2002; Eva *et al*., 2004) differ at the margins from the FAO map; hence estimates of the *total* biomass of Amazonian rainforests will also depend on the spatial extent of forests in different analyses. This topic is not addressed here. For the definition used here, the total extent of Amazonian forests is $5.76 \times 10^6\,km^2$.

The climatic and soils variations across the region were discussed by (Malhi *et al*., 2004). In summary:

(i) There is a general trend of increasing rainfall and decreasing seasonality heading towards north-western Amazonia, but also high rainfall on the eastern Brazilian and Guyanese coasts;
(ii) The El Nino-Southern Oscillation (ENSO) has greatest influence in northern Amazonia, and in particular often leads to episodic droughts in central and eastern Amazonia. ENSO has little consistent influence on rainfall in southwestern Amazonia.
(iii) Sunshine is higher but more seasonal at the northern and southern margins of Amazonia, where the climate shifts towards 'outer tropical' and there are long dry seasons.
(iv) The lowland Amazonian plain consists of low plateaux dissected by river values, and rises very gradually in mean elevation from sea level in the east to 2–300 m a.s.l. in the west. The Brazilian and Guyanese crystalline shield rise to the north and south, with typical elevations of 600–1000 m, and the Andes mountain chain bounds Amazonia to the west.
(v) The most highly weathered soils generally occur in the eastern Amazonian lowlands (Sombroek, 2000), intermediate fertilities are generally found on the crystalline shield regions, and highest fertilities in the Andean foothills, and on sediment-rich floodplains throughout the region. We employ the Cochrane map of soils (www.agteca.com) as our basic soil map. This map does not cover the Guyanas and some sections of eastern Amazonia; for these regions we employed the FAO world soils map. The reclassification of these soil maps into eight basic soil categories is described in a companion paper (Malhi *et al*., in preparation).

[1]Some of the sites presented in Table A1 are estimated to have dry seasons greater than 5 months. This arises from a mismatch between the climatology used for the original FAO map and the climatology we use here – both climatologies are based on sparse data sets and subject to uncertainty in local details. For simplicity where retain the use of the two data sets despite the contradictions at the forest margins.

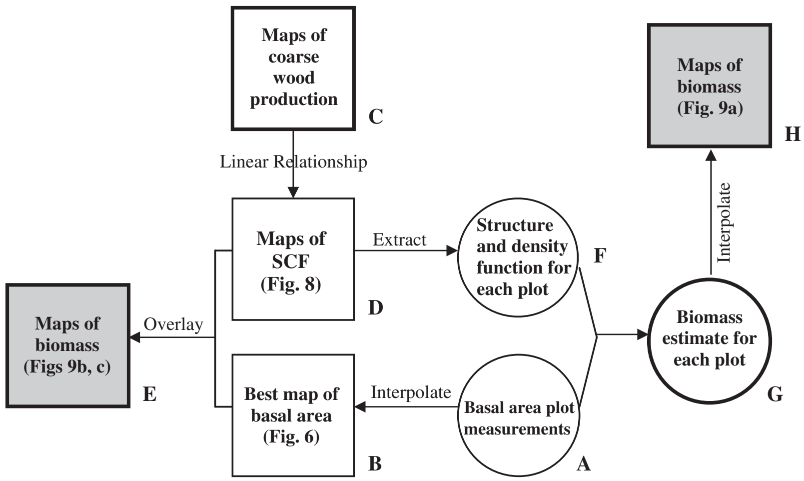


**Fig. 2** A flow diagram indicating the analysis pathways presented in this paper. Squares indicate maps, circles indicates table of values for each plot, shaded squares indicate the end-products: maps of biomass. Details of the analysis pathways are presented in the text.

### *Analysis methodology*

Our approach here, is as follows (letters refer to the flow diagram in Fig. 2):

(1) interpolate the available plot data on basal area per hectare (A) to generate maps of the variation of basal area across South American tropical forests (B);
(2) examine the relationship between biomass, basal area and coarse wood productivity for a subset of plots where these parameters were directly estimated by Baker *et al*. (2004b) and Malhi *et al*. (2004);
(3) apply the relationship derived in (2) to two different maps of wood productivity derived by Malhi *et al*. (in preparation) to produce maps of the structural conversion factor required to convert a basal area measurement to a biomass estimate (D);
(4) directly overlay the map of basal area (B) with the map of the conversion factor (D) to produce a map of biomass (E);
(5) as an alternative approach, use the map of conversion factor (D) to extract the conversion factor for each plot where only basal area information is available (F), and thus, derive an estimate of biomass for each plot (G) and interpolate these to arrive at alternative maps of biomass (H).

Spatial interpolation of the plot data was investigated using three different approaches: kriging, spline interpolation and inverse distance weighting (IDW). Kriging and spline interpolation approaches performed poorly because the high variability of biomass between plots at local scales. Basal area shows considerable local and landscape scale variability (in contrast to productivity, for example, which is dominated by regional-scale variation: Malhi *et al*., 2004). Consequently, the least sophisticated interpolation method (IDW) was found to be most appropriate, and was applied using the geostatistical analysis tool in ArcMAP (ESRI, Redlands, CA, USA). For any value of a continuous variable $B(x, y)$ interpolated between the $N$ neighbouring points $(x_i, y_i)$ in the search window$(i = 1, 2, \ldots N)$, the IDW interpolation at point $(x, y)$ is

$$B(x,y) = \frac{\sum_{i=1}^{N} w_i.B(x_i, y_i)}{\sum_{i=1}^{N} w_i},$$

where

$$w_i = \left[(x - x_i)^2 + (y - y_i)^2\right]^{-p/2}.$$

The power, $p$, is an adjustable parameter that controls the rate of decline of the weighting function. For our purposes the most appropriate setting was $p = 1$: this resulted in a smoothed interpolation with a large number of neighbouring points having some influence, with only a slow decline in weighting function with distance.

## Results

### *Spatial interpolation of basal area*

Our first step is to use the plot measurements of basal area (A in Fig. 2) to produce a best estimate map of basal area (B in Fig. 2). An IDW interpolation of all basal area measurements is shown in Fig. 3a. A feature that stands out is local 'bulls-eyes' driven by individual plots with unusually high or low values. This contrasts with

 

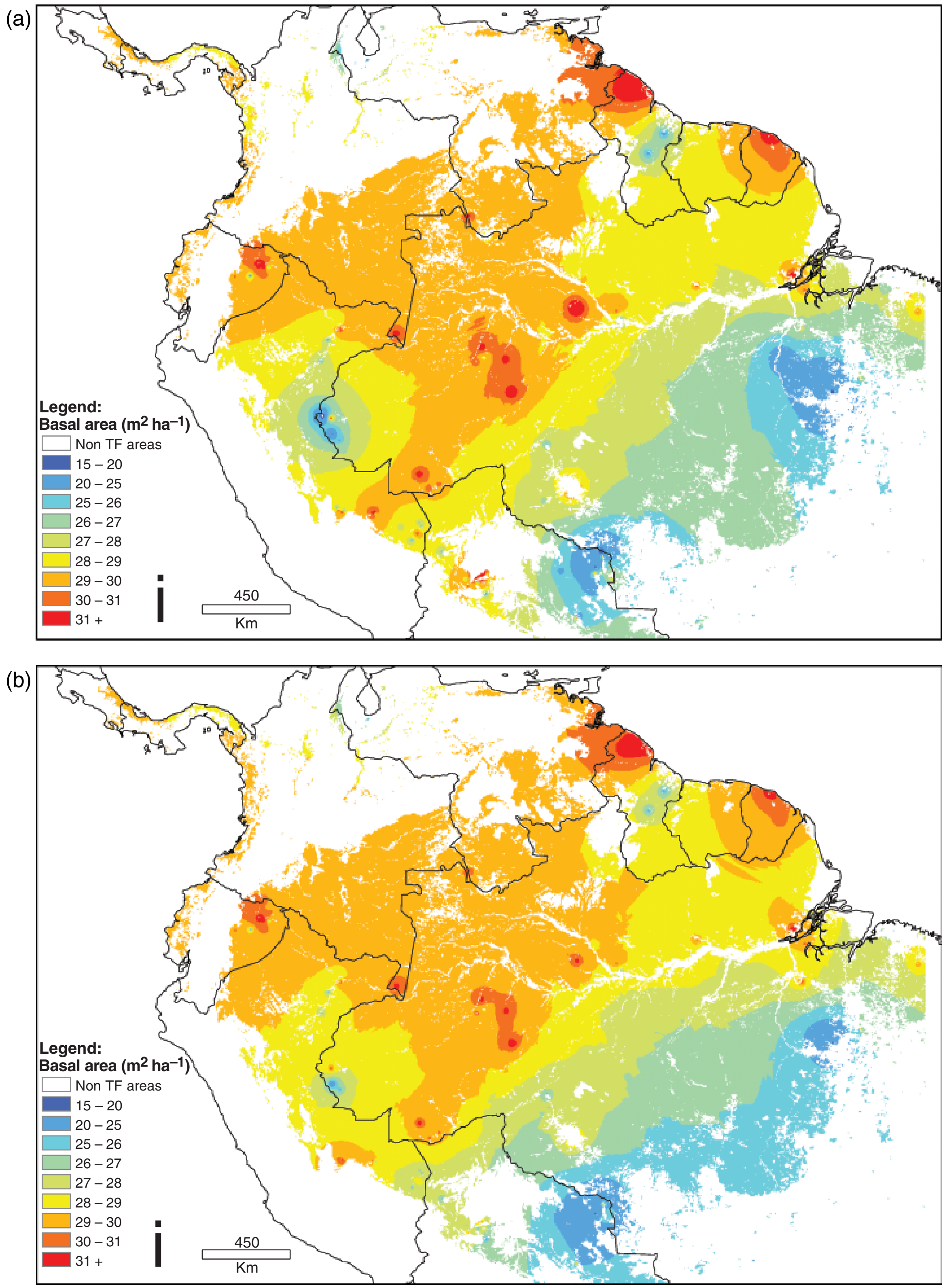


**Fig. 3** (a) A simple interpolation of 227 basal area measurements using inverse distance weighting across lowland South American tropical forests; (b) an interpolation of 199 basal area measurements (28 plots have been removed as 'outliers' – details given in the text).

maps of forest productivity, which are much smoother. This feature arises because basal area is much more affected by local landscape features (e.g. local topography, or recent natural disturbance) and such local variations can swamp regional patterns. In addition, 1 ha sample plots may not be large enough to accurately sample the variance in biomass introduced by large trees (Chave *et al.*, 2003), but may be sufficient for assessment of wood productivity, as evidenced by the greater similarity in wood productivity values between neighbouring plots (Malhi *et al.*, 2004).

As our interest here is to examine broad regional patterns, we employed a filter to remove locally anomalous plots and smooth the data set. The approach identified clusters of forest plots (of varying sizes) and local anomalous plots were removed if the value for the plot fell outside the range (mean value of neighbours $\pm$ standard deviation of neighbouring values $\times$ threshold), where the threshold was varied between values of 1.0 and 1.8.

The effect of removing anomalous plots is shown in Fig. 4. Removing outliers improves the predictive power of the interpolation (as would be expected), but with greater data removal there is greater danger of losing genuine regional variation. We adopted a compromise approach of using a search radius of 250 km and a threshold value of 1.6 for anomaly removal. This corresponds to an inflection in Fig. 4 which indicates an optimal compromise between a significant improvement in predictive power and minimum data shedding. This removes 28 plots (12% of plots; removed plots are indicated with an asterisk in Table A1), and improves the cross-validation statistics by 22%. The interpolated may of basal area with outliers removed is shown in Fig. 3b. The 'bulls-eye' pattern has reduced in intensity, although not disappeared completely.

The relationship between basal area and climatic variables was explored by cross-correlation analysis (Table 1). The cross-correlations were significantly improved by the removal of locally anomalous plots. The strongest correlation (−0.38) was found to be with dry season length and/or total annual rainfall (these two climatic variables were strongly correlated), and this relationship was explored further.

Figure 5 plots the basal area against dry season length. There is substantial site-to-site variability, indicating that local landscape controls dominate over regional trends. There is little evidence of any relationship for moderate seasonality (less than 4 months dry season), but evidence of a general decline in the basal area of tropical forests with increasing water stress for longer dry season lengths. This is to be expected as root competition for dry season water resources intensifies, and the ground surface is able to support less stem water uptake per unit area (e.g. Meinzer *et al.*, 1999).

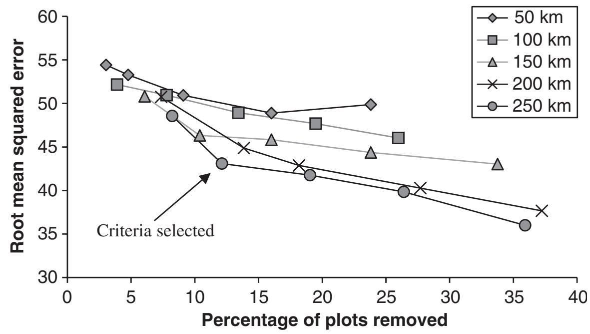


**Fig. 4** The root mean squared error value obtained by cross validation of inverse distance weighting interpolations of basal area, plotted against the percentage of local anomalous plots removed using different thresholds for outlier identification. The different lines represent different sized search radii employed by the outlier identification algorithm. The arrow indicated the selected optimum outlier removal procedure (threshold = 1.6, search radius = 250 km), a compromise between maximizing error reduction and minimizing data shedding.

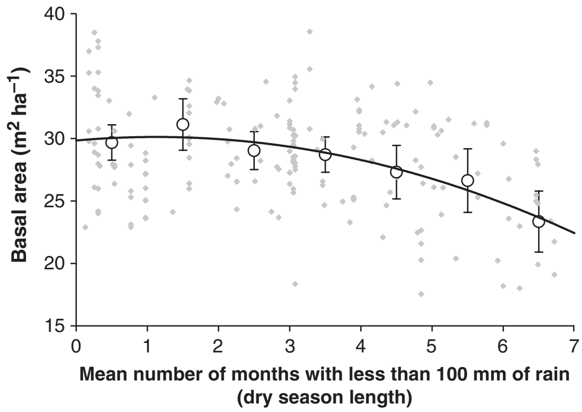


**Fig. 5** Plot measurements of basal area (with 28 local outlier plots removed) plotted against dry season length. Grey diamonds indicate individual plot data, open circles are binned means, error bars are 95% confidence limits. The polynomial trend line is fitted through the binned means: $y = -0.22x^2 + 0.50x + 29.84$ ($r^2 = 0.93$). A polynomial fit through individual points is almost identical: $y = 0.29x^2 + 1.00x + 28.87$ ($r^2 = 0.18$).

A revised interpolation of basal area with dry season length factored in (Fig. 6) was conducted by calculation of a smooth mean basal area field from the basal area–dry season length relationship in Fig. 5, and then IDW interpolation and superposition of the residuals of each data point relative to this mean field. There was no significant correlation between the residuals and any other climatic variable. The major difference from Fig. 3

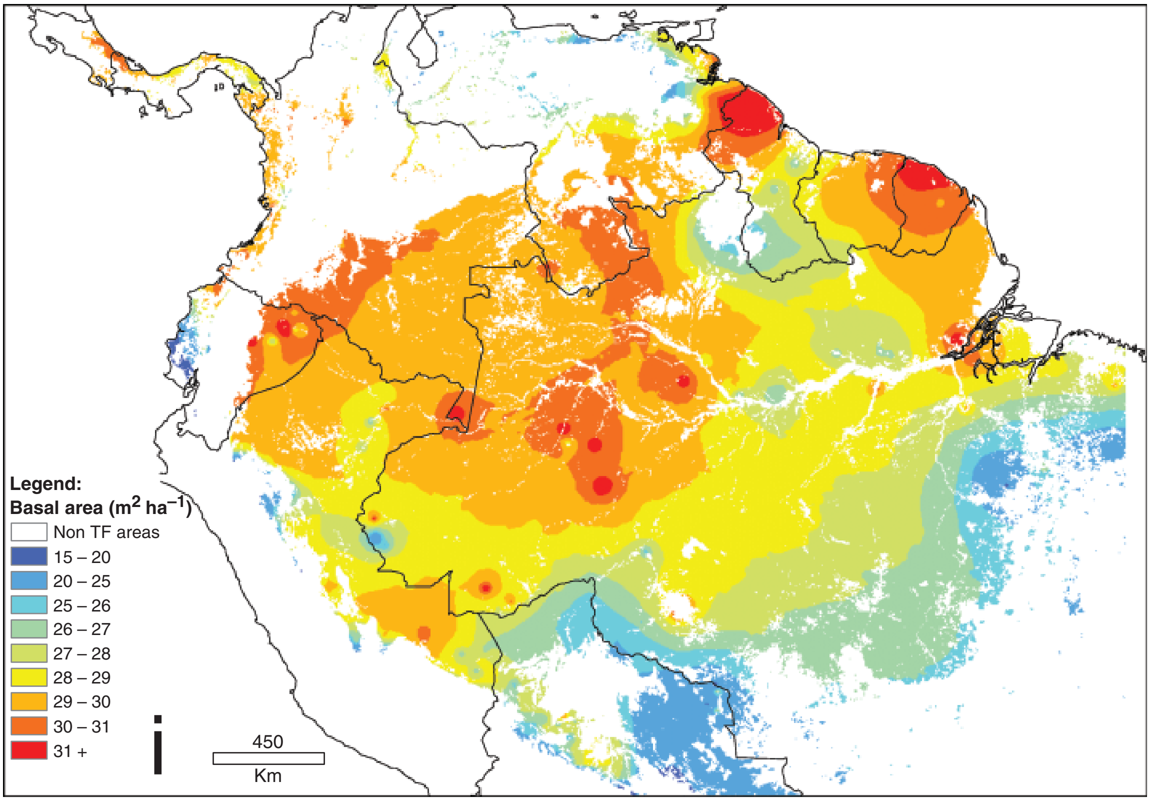


**Fig. 6** An interpolation of forest basal area across lowland South American tropical forests incorporating the relationship with dry season length described in Fig. 5 (with 28 local outlier plots removed).

is in south-eastern Amazonia, where there is a paucity of field plots. This extra information gained from incorporating dry season length into the model suggests that the wetter forests extend further into this region than suggested by direct spatial interpolation of plot data, and hence, basal area in this region is higher than expected. Another feature is a reduction of predicted basal area in the dry region in the central Guyanas, which is consistent with the available plot data in the region. We consider this interpolation to be our current best estimate of the spatial variation of basal area in Amazonia.

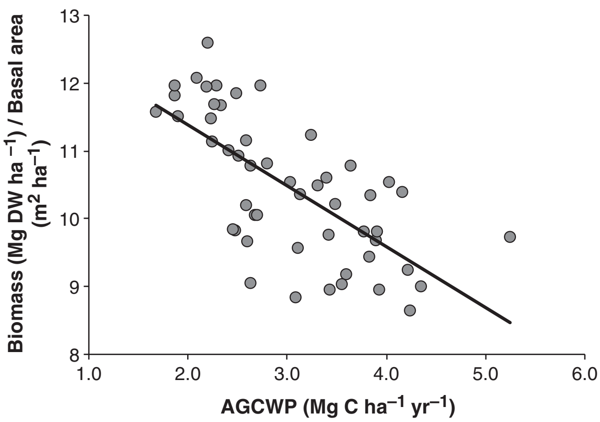


**Fig. 7** The relationship between the structural conversion factor, SCF ( = plot aboveground live biomass/plot basal area) and aboveground coarse wood productivity for 56 lowland Amazonian forests. Biomass and basal area values are derived from Baker *et al*. (2004), productivity values from Malhi *et al*. (2004). The least-squares linear fit (black solid line) is $y = -0.90x + 13.19$, $r^2 = 0.48$.

## *Structural and density factor*

Our next step is to relate basal area to biomass. We will refer to the ratio between aboveground live biomass (of trees >10 cm dbh) and basal area (i.e. the mean amount of biomass supported per unit of forest basal area) as the structural conversion factor (SCF). Baker *et al*., (2004b) found that variations in wood density and size class distribution have a significant influence on the SCF, and that spatial variations in SCF appeared more important than variations in basal area in determining the spatial pattern in aboveground biomass. Figure 7 demonstrates that the SCF is related to wood productivity, with more productive forests having lower wood density. There is, however, some variance that is not related to wood density, and is instead influenced by size-class distribution.

Using the relationship shown in Fig. 7, we mapped the spatial variation in the SCF (D in Fig. 2) using the maps of wood productivity generated in Malhi *et al*. (in preparation; C in Fig. 2). Two productivity maps were used: one that was a direct kriging interpolation of the productivity data, and a second based on a 'painting-by-numbers' approach (Schimel & Potter, 1995) that assumed productivity was related to soil type (both maps are shown in Fig. 8). Details of the extrapolation of productivity data will be given in Malhi *et al*. (in preparation). The SCF varies by about 30%, between 9 and 12 Mg DW $m^{-2}$ basal area. Both maps show a similar broad regional pattern with lower SCF being found in the more dynamic western Amazonian forests, and high values in north-east Amazonia. The two maps differ in smoothness and in detail. If the spatial variability is predominantly driven by soil prperties (Malhi *et al*., 2004), the map suggests that the highest values of SCF are found in the old, highly weathered oxisols along the main Amazon valley, and intermediate values are to be found on the crystalline shield to the north and south. The soils-based map gives spatial details but the consistency of the SCF : soil relationship and the local details of the soils map are still uncertain, so these local details should be treated as tentative. The calculations in the rest of this paper will be based in parallel on both the kriging and soils-based interpolations. The basal area and SCF show almost no spatial correlation and can be treated as independent influencing factors on biomass (the correlation coefficient between plot values of basal area and kriging-derived SCF was 0.02; between basal area and soils map-derived SCF it was −0.05).

### *Maps of biomass*

Having derived maps of basal area (B in Fig. 2) and SCF (D in Fig. 2), our next step was to estimate the SCF and biomass for each plot (F and G in Fig. 2). Where plot biomass had been directly derived from the individual tree data using a consistent protocol as described by Baker *et al*. (2004b), this value was preferred. Where such directly calculated biomass was not available, we extracted an estimate of SCF for each plot from the maps in Fig. 8, and multiplied this by the reported basal area to calculate the plot biomass. These values are listed in Table A1.

We then employed three approaches to produce region-wide maps of biomass:

1. Use the allometric relationship derived for the central Amazon with no allowance for spatial variation in SCF.
2. Directly overlay the maps of basal area (B in Fig. 2) and the maps of the SCF (with one map each for the kriged and soil-based interpolations; D in Fig. 2) to produce a map of biomass (E in Fig. 2).
3. Directly interpolate the derived biomass values for each site (G in Fig. 2) to produce an alternative map of biomass (H in Fig. 2). We used the same procedure and thresholds to remove local anomalies as outlined for the basal area interpolation above.

The resulting maps of biomass are shown in Fig. 9. There are significant differences in details between the kriging-based and soils-based maps, but the overall patterns are similar. The two different routes to calculating biomass (E and H in Fig. 2) yield very similar results, with the exception that H does not factor in the relationship between basal area and dry season length. Hence, we consider Fig. 9b and c to be our best estimates of forest biomass. In general, biomass is calculated to be highest in central Amazonia and on the Guyana coast. This represents an optimum combination of high basal area (related to short dry season length) and high wood density (related to low productivity and probably to infertile soils). As we head to aseasonal northwestern Amazonia, basal area increases but is offset by the increasing abundance of low wood density species. Heading towards the dry southern and northern margins, wood density is moderately high, but basal area drops off because of limited water availability. The coastal areas of Brazil and the Guyanas also appear to have high biomass, a combination of the high basal area sustained by oceanic front rainfall, and high wood density on infertile soils. Comparing the soils-based map (9c) with the kriging map (9b), the soils map suggests that the high wood density zone may extend further northwest into the infertile soils of lowland Colombia and Venezuela, and snake east along the lowland corridor bordering the Amazon river, but the broad patterns are similar. Overall, regional mean biomass over the forest area of $5.76 \times 10^6$ $km^2$ varies between 250 and 350 Mg DW $ha^{-1}$ $yr^{-1}$. The mean value reported by Baker *et al*. (2004b) was 298 ($\pm$51) Mg DW $ha^{-1}$, suggesting that the core dataset used by Baker *et al*. (2004b) was well distributed.

The per hectare and total carbon stocks (over area $5.76 \times 10^6$ $km^2$) for the lowland Amazonian forests calculated by the different approaches are tabulated in Table 2. The most apparent feature is that incorporation of spatial variability in the SCF reduces the estimated total carbon stocks by about 8% from 92 to 83–86 Pg C (top row vs. bottom two rows). This is because the default allometric relationships used are based on studies in the central Amazon near Manaus, a region shown in Fig. 9 to have among the highest biomass

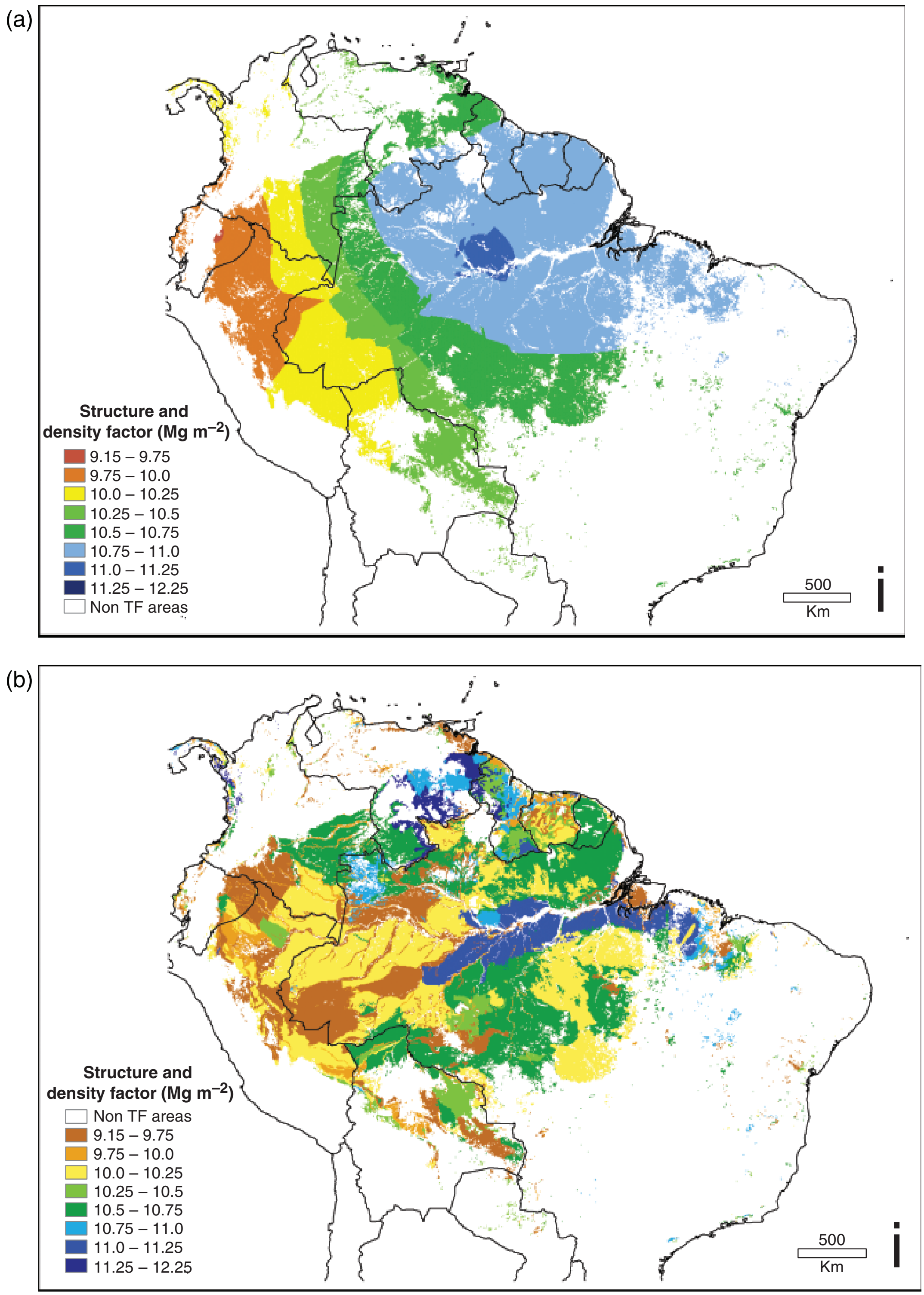


**Fig. 8** Interpolation of the structural conversion factor across lowland South American tropical forests derived using the linear relationship presented in Fig. 7 with (a) a map of aboveground coarse wood productivity (AGCWP) interpolated by ordinary kriging, and (b) a map of AGCWP based on soil categories.

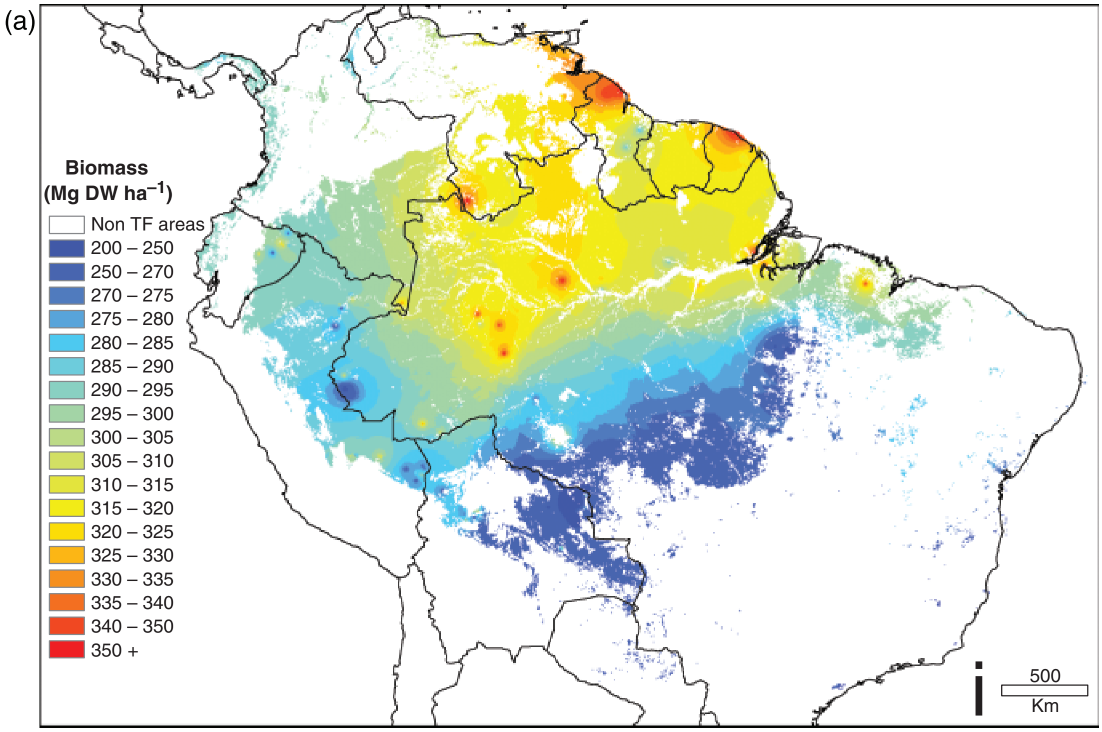


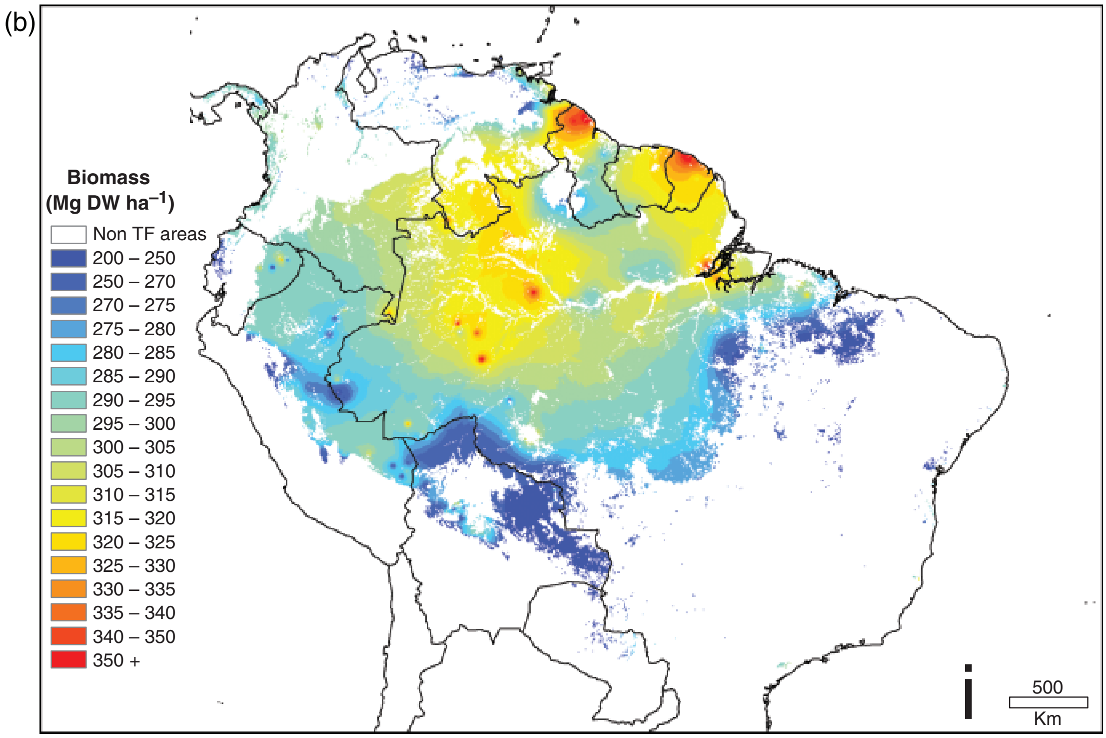


**Fig. 9** Interpolations of biomass of lowland South American tropical forests: (a) calculated by interpolating biomass estimates generated at each plot (with 25 local anomalous plots removed using a search radius of 250 km) using inverse distance weighting ( = Box H in Fig. 2); (b) calculated by overlaying the best basal area estimate (Fig. 6) with maps of the structure and wood density function (Fig. 8), using kriged interpolations for both maps ( = Box E in Fig. 2); (c) as for (b) but using soils-based interpolations instead of kriged interpolations.

 

values in Amazonia. The particular method of spatial interpolation used has little effect on estimates of total biomass: the soils-based interpolations (bottom row) tend to give a value 2–3% lower because they suggest that poorly sampled regions of the Amazonian crystalline shield may have high fertility and lower wood density than simple kriging of the existing plot data would suggest.

The values cited here are for aboveground woody biomass of all live trees >10 cm dbh. To arrive at total biomass carbon stocks we need to include a number of extra terms, such as the biomass of trees <10 cm dbh, the biomass of lianas, dead biomass, and belowground carbon. These extra terms have been estimated for some forest plot sites, but as their spatial variation is unclear we do not attempt to map their spatial variability, but rather include mean values as multiplicative factors to arrive at estimates of total biomass carbon stocks. To be consistent with Phillips *et al*. (1998), we estimate the biomass of trees less <10 cm to be an additional 6.2%, based on forest plots in the Manaus region, and the biomass of lianas to be 3.7% of total aboveground tree biomass, based on several plots in western Amazonia. Dead wood biomass has been estimated at a number of sites and ranges between $6.4 \pm 1.6\,\mathrm{Mg\,C\,ha^{-1}}$ over 10 ha in southern Peru (Baker *et al*., submitted) and 25–30 $\mathrm{Mg\,C\,ha^{-1}}$ at two sites in eastern Amazonia (Keller *et al*., 2004; Rice *et al*., 2004), and Houghton *et al*. (2001) report a mean value of 10% of live biomass, the value that is applied here. Belowground biomass has been measured at only a few sites, and Houghton *et al*. (2001) report a mean value of 21% (range 13–26%) of aboveground live tree biomass; that value is applied here. Applying these approximate multiplicative factors uniformly to our previous estimate of aboveground live woody biomass (83–86 Pg C), we estimate that the total aboveground live woody biomass is about 91–95 Pg C, the total aboveground woody biomass is about 100–104 Pg C, and the total woody biomass is 121–126 Pg C.

## Discussion

Using data from 227 forest plots, we have explored the spatial variation of aboveground live biomass in Amazonia, with particular emphasis on accounting for variations in basal area and wood density. Although there is substantial site-to-site variability, we were able to determine the somewhat opposing trends in these two factors, both of which are important determinants of AGLB. Wood density tends to peak in the slow growing forests on infertile soils in eastern lowland Amazonia and the Guyanas, and is lowest in the much more dynamic forests of western Amazonia. Basal area generally declines with increasing dry season length, for regions with a 4 months or longer dry season. The superposition of these two factors indicates that biomass is highest in central Amazonia and the Guyanas, and is about 15% lower in the more dynamic west, and lowest in the dry fringes to the south and north.

The estimates of aboveground live biomass were based on two parameters: basal area and structural conversion factor. These two parameters seem fairly independent at regional scales – basal area is related to hydraulic considerations and hence to dry season length, whereas the structural conversion factor is related to productivity and hence probably to soil fertility (Malhi *et al*., 2004). The combination of these two factors leads to maximum biomass is wet regions with low wood productivities and infertile soils, such as central Amazonia and the Guyana coast, and lower biomass in dynamic western Amazonia, and the dry southern and northern fringes.

A number of the removed 'anomalous plots' show evidently unusual properties (e.g. the liana-dominated forests at CHO-1 CHO-2, XIN-01 and XIN-02, the bamboo-dominated forests RES-06 and CAM-02, fire-affected forest at NKT-01 and NKT-02, the gallery forests NKE-02, NKG-01). While these obviously influence regional analyses of biomass, it is not surprising that the ecological and/or historical factors that cause their unusual properties are not captured in this broad analysis. Other forest plots are suspected of being subject to a majestic forest sampling bias where the original investigators deliberately selected high biomass stands (e.g. BEN-5, BEN-10, BEN-9: 'contains one of the last remaining stands of *Swietenia macrophylla* in the reserve reaching seven trees per hectare'). Others may be recently affected by a local natural disturbance (BDF-04 suffered recent high mortality from a La Niña-related flooding event). A number of the anomalous sites have no obvious explanation, which may reflect the random influence of a single very large tree within the sample plot, or our ignorance of detailed sampling methodologies, or else additional factors that are not considered in this analysis.

### *Uncertainties*

*Tree height allometry.* Probably the most important factor that has not been included here is spatial variability in height allometry, which would be expected to show a similar pattern to basal area and decrease with increasing dry season length as hydraulic constraints on tree height become more severe. Hence, biomass would drop off more rapidly at the dry extremes. However, it is not clear whether height allometry shows any variation under moderate dry season conditions, and hence, whether the central Amazonian peak in biomass would be shifted towards more aseasonal regions.

*The relationship between wood density and allometry.* In adopting the approach of Baker *et al*. (2004b), we are assuming that allometries can be scaled linearly by wood density. It is plausible that low wood density trees have different architecture than high wood density trees. However, in their comprehensive assessment of tree allometry of 2410 trees, Chave *et al*. (2005) found that their null hypothesis of a linear relationship between wood density and aboveground biomass was not rejected, suggesting there is little evidence of a nonlinear scaling by wood density. Moreover, Chave *et al*. (2005) found no significant difference in allometries from South American and South-East Asian forests (constructed by lumping all species), despite the fact that these forests share almost no common genera, and very different dominant families. This again suggests no significant allometric differences between major tree dicot families.

*Biased land-form selection.* There may be some biases in site selection in our plot network (e.g. plateaux are favoured over steep slopes, accessible flood plains are favoured over 'interior' forests). In the soils-based interpolation, we try to account for landform using by including the various 'facets' in the Cochrane and FAO maps (e.g. if the map described a land form as 90% plateau, 10% river valley, these are assigned different values). Given that there is little difference between the soils-based and kriging interpolations in *total* biomass, it is unlikely that our estimate in total biomass will be strongly affected by this bias, although the details of regional patterns may vary. A remote sensing analysis to evaluate the landscape context of a number of the RAINFOR plots is currently under way.

*Biased sampling of disturbance-recovery dynamics.* Old growth tropical forests have a natural disturbance-recovery dynamic (e.g. sites are hit by occasional large tree falls/blowdowns, followed by slow recovery in biomass until the next infrequent disturbance). In setting up forest plots, it is possible that sites that recently underwent strong natural disturbance (e.g. storm blowdowns) were avoided. The would lead to an overestimate of the background biomass of old-growth forest biomass. The magnitude of such a bias is likely to be small, but is difficult to quantify and requires detailed exploration of the disturbance-recovery dynamics of Amazonian forests.

*The effect of wrinkled topography.* Most of the forest plots are established in terms of a fixed ground area. In regions of significant slopes or undulating topography, the biomass per unit area of the Earth's surface could be significantly higher. This 'wrinkled topography' effect would increase biomass estimates in geomorphological transition zones such as the periphery of the Andes, and the Brazilian and Guyanan shields. It should be straightforward to estimate this effect with high-resolution digital elevation data.

### *Quantification of uncertainty in region-wide totals*

The above sources of uncertainties in our biomass totals can be classified into two categories (Chave *et al*., 2004): sampling uncertainties caused by partial sampling of a landscape that is heterogeneous at many scales, and systematic biases caused by errors in methodology of biomass measurement or analysis, such as incorrect allometric equations. Stochastic sampling uncertainties in our estimates of biomass are likely to be smaller when considering basin-wide totals, as opposed to accurate prediction of biomass at specific sites. Table 2 gives us some insight into the likely sensitivity of basin-wide totals to sampling uncertainties:

(i) The total area of forest sampled (excluding the 50 ha Panama site) is 366.1 ha, which can be divided into approximately seven regions of 50 ha each. The standard error of mean basal area over the entire dataset is about 1% (over each region it is about 4%). With a normal distribution, the 95% confidence limits would be 2% and 8%, respectively. This is consistent with the findings of Keller *et al*. (2001) and Chave *et al*. (2003), who reported that approximately ten 1 ha plots are required to bring 95% confidence limits within 20%, and 26 ha to bring these limits within 10%. Assuming well-distributed sampling, the random sampling uncertainty in basin-wide and regional basal area estimates would be 2% and 8%, respectively (95% confidence).

(ii) Uncertainty in the use of allometric models contributes a systematic uncertainty of about 13% (Chave *et al*., 2005).

(iii) Imposition of the SCF reduces estimates of total regional biomass by 7%; the variation in assumption about the exact distribution of SCF causes a systematic bias of about 3% in final biomass (rows in Table 2b).

(iv) Similarly, removal of outliers, and comparison with the mean of the sample plots has only modest influence on basin-wide totals, of order 3% (columns in Table 3b). This suggests that the spatial sampling bias contributes an uncertainty less than 5% in basin-wide totals.

**Table 2** The aboveground live biomass of trees >10 cm diameter for all lowland Amazonian forests, as calculated by different interpolation procedures: (a) mean dry-weight per hectare (Mg DW $ha^{-1}$); (b) summed over the forest area and converted to carbon units (Pg C). The columns correspond to (left to right): (i) the overlay of the basal area interpolation (with 28 outliers removed) with the structural conversion factor; (ii) direct interpolation of plot biomass estimates with no outliers removed; (iii) direct interpolation of plot biomass estimates with 28 outliers removed

| | Biomass calculated from the BA interpolation based on DSL (Mg DW $ha^{-1}$) | Biomass values calculated at individual plots* and then interpolated using IDW | |
|---|---|---|---|
| | | No plots removed (Mg DW $ha^{-1}$) | Plots removed (Mg DW $ha^{-1}$) |
| (a) | | | |
| ASSUMPTION SCF | | | |
| None | 320 | X | X |
| Derived from ordinary kriging of AGCWP | 298 | 297 | 297 |
| Derived from soil type classification of AGCWP | 289 | 289 | 291 |

| | Biomass calculated from the BA interpolation based on DSL (Pg C) | Biomass values calculated at individual plots* and then interpolated using IDW | |
|---|---|---|---|
| | | No plots removed (Pg C) | Plots removed (Pg C) |
| (b) | | | |
| ASSUMPTION SCF | | | |
| None | 92.4 | X | X |
| Derived from ordinary kriging of AGCWP | 85.8 | 85.5 | 85.7 |
| Derived from soil type classification of AGCWP | 82.9 | 83.3 | 83.8 |

The rows correspond to different assumptions about the variation of SCF (top to bottom): (i) SCF fixed at values for central Amazonia; (ii) kriged interpolation of SCF (Fig. 8a); (iii) soils-based interpolation of SCF (Fig. 8b).

(v) Other uncertainties listed above are currently more difficult to quantify, but in total they are unlikely to exceed 10%.

If all these uncertainties were strongly correlated, the total uncertainty in biomass estimates would be about 35%, if they were independent the total uncertainty would be 18%. Hence, 25% is a conservative estimate of uncertainty in basin-wide biomass totals, with systematic uncertainty in allometric relationships being the biggest contributing factor. Applying an uncertainty of 25% to our previous calculations, we estimate that the total aboveground live woody biomass is $93 \pm 23$ Pg C, the total aboveground woody biomass is about $102 \pm 26$ Pg C, and the total woody biomass is $123 \pm 31$ Pg C.

### *Comparison with previous estimates for Brazilian Amazonia*

How does our estimate of the spatial patterns and total biomass of Amazonian forests compare with previous estimates? Houghton *et al*. (2001) compared a variety of maps of biomass for the Brazilian Amazon only. From our study mean biomass values were extracted from Fig. 9 for forested regions of the Brazilian Amazon only (area $3.60 \times 10^6$ $km^2$ compared with total Amazonian forest area $5.76 \times 10^6$ $km^2$), and these are presented in Table 3 for comparison with various values reported by (Houghton *et al*. (2001). For compatibility, the 30% correction that Houghton *et al*. applied for dead wood and below-ground biomass has removed, (i.e. we are considering aboveground live biomass only). A 10.1% correction for trees <10 cm dbh and lianas has been retained for our analysis to be compatible with Phillips *et al*.(1998). For the field measurements summarized by Houghton *et al*. (2001), it was not clear which data sets included small trees and lianas, and which did not.

Allowing for regional variations in basal area and SCF, we calculate the mean AGL biomass of Brazil Amazonian moist forests to be about 160 Mg C $ha^{-1}$ (6–10% lower than if a central Amazonian structure factor had been uniformly applied), with a 25% uncertainty as discussed above. This is close to the value of 148 Mg C $ha^{-1}$ that Houghton *et al*. (2001) extrapolated from 44 sites. Many of these sites did not account for

 

**Table 3** (a) The mean above-ground live biomass of trees in lowland forests *in Brazilian Amazonia only*, including a 10.1% correction factor for small trees and lianas

| | Biomass calculated from the BA interpolation based on DSL ($Mg\,C\,ha^{-1}$) | Biomass values calculated at individual plots and then interpolated using IDW | |
|---|---|---|---|
| | | No plots removed ($Mg\,C\,ha^{-1}$) | Plots removed ($Mg\,C\,ha^{-1}$) |
| (a) | | | |
| ASSUMPTION SCF | | | |
| None | 175 | X | X |
| Derived from ordinary kriging of AGCWP | 164 | 163 | 163 |
| Derived from soil type classification of AGCWP | 158 | 157 | 159 |

| Study | Total Biomass ($Mg\,C\,ha^{-1}$) | Above-Ground Live Biomass: No small trees ($Mg\,C\,ha^{-1}$) | Above-Ground Live Biomass: With small trees ($Mg\,C\,ha^{-1}$) |
|---|---|---|---|
| (b) | | | |
| Houghton interpolation of 44 points | 192 | 148 | 163 |
| RADAMBRASIL (Brown *et al*., 2002) | 156 | 120 | 132 |
| RADAMBRASIL (Fearnside, 1997) | 232 | 141 | 155 |
| Brown (calibrated with 39 of 44 points) | 183 | 141 | 155 |
| Brown (calibrated with forest surveys) | 196 | 151 | 166 |
| Brown (calibrated with areas >0.5 ha) | 197 | 152 | 167 |
| Olson | 100 | 77 | 85 |
| Potter | 196 | 151 | 166 |
| DeFries | 178 | 137 | 151 |
| This study | | 143–149 | 157–164 |

For comparison reasons, values are presented in carbon units $Mg\,C\,ha^{-1}$. Columns and rows describe different analysis procedures as in Table 2. (b) The total biomass and above-ground live biomass of trees in Brazilian Amazonia, for various studies summarised by Houghton *et al*. 2001, in $Mg\,C\,ha^{-1}$. The last column includes a 10.1% correction for small trees and lianas, as explained in the text.

small stems or lianas – once this 10.1% correction is applied to the Houghton *et al*. (2001) estimate the two values are very similar. In spatial detail the Houghton *et al*. (2001) extrapolation picks out some of the broad features that are confirmed with greater confidence in our (more data-rich) estimate: high biomass in the central Amazon and low values at the dry fringes.

Houghton *et al*. also report estimates of Brazilian Amazon biomass from a number of other field and model studies. These are compared briefly with our estimates:

*Estimates derived from RADAMBRASIL.* The RADAMBRASIL project (DNPM, 1973–1983) made an inventory of stemwood volumes on thousands of 1 ha old-growth forest plots across Brazilian Amazonia, measuring stems >31.8 cm dbh, providing the most spatially intensive and systematic Amazonian forest inventory to date, albeit constrained by sampling only medium and large trees. Brown & Lugo, (1992) and Fearnside, (1997) used standard structure factors to convert to these data to biomass with a uniform wood density of $0.69\,g\,m^{-2}$. The two studies differed in that Fearnside tried to include additional terms, such as small trees <10 cm dbh (+12%), lianas (+5.3%), palms (+2.4%), hollow trees (−6.6%) and bark (−0.9%). In addition, Fearnside also estimated high values for belowground biomass (33.6% of AGL biomass) and dead biomass (31% of AGL biomass), leading to estimates of total forest biomass some 60% higher than those of Brown and Lugo. These total biomass values seem at the high end of the range of values reported from field studies, but for below-ground biomass do take into account aspects that are frequently neglected, such as below-ground boles and tap roots. Considering AGL biomass alone, Fearnside arrives at a mean value for Brazilian Amazonia of $141\,Mg\,C\,ha^{-1}$, a value close to that reported here, compared with $120\,Mg\,C\,ha^{-1}$ by Brown & Lugo (1992).

One noticeable feature is that the RADAMBRASIL based maps do not indicate the peak in biomass in central Amazonia as strongly the present study, although there is some indication of lower biomass at the dry fringes. One possible reason for the attenuation of this trend is that the RADAMBRASIL survey sampled only medium and large trees (>31.8 cm dbh). Although total basal area appears to decline with increasing dry season length (and this is also consistent with physiological water-use principles), mean tree size increases with dry season length (Malhi *et al*., 2002) (i.e. the decline in basal area is disproportionately in small trees, which were not sampled by RADAMBRASIL).

*Brown and Lugo estimates*. Brown and colleagues have advanced a method for estimating potential biomass of tropical forest lands that takes into account variation in four environmental parameters: soil depth, texture, elevation and slope. Details of the approach are given in Houghton *et al*. (2001), but in summary the approach was calibrated off either 39 sites (mainly of area <0.5 ha), or six large FAO inventories, or 16 sites where the area sampled was greater than 0.5 ha. The three approaches yield a value of AGLB in Brazilian Amazonia between 141 and 152 Mg C $ha^{-1}$. These extrapolations indicated highest biomass in western Amazonia, in disagreement with the present study, but are based on very few points.

The classic study by Olson *et al*. (1983) of biomass for 44 terrestrial ecosystems yields estimates half the size of all other reported values, and are likely to be in error. *The NASA-CASA model* (Potter, 1999) yields a mean value of AGLB in Brazilian Amazonia of 151 Mg C $ha^{-1}$, but with biomass increasing in drier regions, the opposite of what is observed. The mechanism for this discrepancy clearly requires further investigation, but is likely to be related to the calculation of wood productivity and residence time.

## Conclusions: Uncertainties and Future Directions

We have explored the spatial variation of aboveground live biomass in old-growth Amazonian forests, with particular emphasis on accounting for variations in basal area and wood density. Our estimates covered all of Amazonia, but we were able to compare the results from Brazilian Amazonia with previous estimates, which are based either on a smaller number of inventories, or on the extensive but less complete RADAMBRASIL inventories, or on modelling and satellite-derived studies. Although our estimates were comparable in mean values with most previous estimates, they often differed in the spatial distribution of biomass. These discrepancies can be explained by:

(i) the greater size of the data set presented here compared with other small-plot-based extrapolations, which enabled clearer definition of trends in basal area;
(ii) accounting for wood density and its relationship with forest dynamism, which enabled tracking of the decline in biomass to the west;
(iii) accounting for trees >10 cm and <31.8 cm dbh (in contrast to the RADAMBRASIL surveys), which indicated a decline in basal area at the dry fringes.

Two hundred and twenty-six plots is still a small number compared with the extent of Amazonia, and the details of the maps presented in Fig. 9 are likely to be modified as data sets expand. The main intent of this paper is to identify principles that need to be accounted for in future estimates of biomass:

(1) Forest basal area in relatively invariant at about 30 $m^2$ $ha^{-1}$ at regional scales in moist Amazonian forests, but declines in drier areas.
(2) This regional-scale invariance in mean basal area occurs despite a threefold variation in regional wood productivity (Malhi *et al*., 2004).
(3) *K*–*r* tradeoffs between high wood density, long-living species and low wood density, short-lifetime species lead to a regional variation in wood density that significantly affects regional patterns of biomass. Hence, ecological interactions, that are not incorporated in current biogeochemical approaches to estimating forest carbon stocks, are important determinants of forest biomass.
(4) The trends in basal area and wood density have somewhat opposite directions, resulting in the highest forest biomass regions occurring in central Amazonia and the Guyana coast.
(5) There is no simple correlation between biomass and wood productivity, and the two should not be confounded.

Uncertainties that remain include the following issues:

(i) The variation of tree height (and hence wood volume) with environmental factors is poorly described. This could be tackled through both field surveys and remote sensing approaches (e.g. lidar altimetry)
(ii) We have produced two 'final' maps of biomass, reflecting that the apparent relationship between wood density and soil fertility is still tentative. There is a clear need to explore the relationship in more detail with improved soil data sets, such as those recently collected by the RAINFOR project. If soil fertility is indeed the controlling factor for wood productivity and hence density, an obvious next step is the identification of which soil fertility

 

parameters are key (e.g. soil texture, phosphorus availability, pH, cation exchange) and mapping of their spatial variation.

(iii) There are major gap regions in the dataset, such as the southern dry margins of Amazonia, the crystalline shield regions, and much of Colombia. These need to be filled, through further 'mining' and compilation of existing datasets, or targeted field studies.

(iv) The approach we apply explores regional-scale variation in biomass, but only weakly addresses landscape scale variation (variation of wood density with landform facet is accounted for, but variation in basal area is not). Local variation clearly dominates estimates of basal area at the hectare scale. It should be also possible to account for landscape-scale variation (e.g. slope, soil depth), perhaps using an approach similar to (Brown & Gaston, 1995).

(v) We have generated a map of biomass of old-growth forests as an upper envelope of estimates of biomass of the complete Amazonian forest disturbance mosaic. To arrive at a map of actual forest biomass, it is necessary for data on secondary forests, logged forests, and natural disturbance-recovery dynamics, be superimposed on this map to arrive at estimates of actual forests biomass.

An obvious next step is to combine the ecological insights presented here with the wealth of new remote sensing information and analyses becoming available, to conduct extrapolations that explicitly include remotely-sensed information on landscape context, forest structure, and forest disturbance.

## Acknowledgements

We thank Ailsa Allen for her assistance with figure preparation. Development of the RAINFOR network, 2000–2002, was funded by the European Union Fifth Framework Programme, as part of CARBONCYCLE-LBA, part of the European contribution to the Large Scale Biosphere-Atmosphere Experiment in Amazonia (LBA). RAINFOR field campaigns were funded by the National Geographic Society (Peru 2001), CARBONCYCLE-LBA (Bolivia 2001) and the Max Planck Institut für Biogeochemie (Peru, Bolivia 2001, Ecuador, Brazil 2002, Brazil 2003). We gratefully acknowledge the support and funding of numerous organisations who have contributed to the establishment and maintenance of individual sites: in Bolivia, U.S. National Science Foundation, The Nature Conservancy/Mellon Foundation (Ecosystem Function Program); in Brazil (SA) Conselho Nacional de Desenvolvimento Cientifico e Tecnológico (CNPq), Museu Goeldi, Estacão Cientifica Ferreira Penna, Tropical Ecology, Assessment and Monitoring (TEAM) Initiative; in Brazil (SGL, WFL), NASA-LBA, Andrew W. Mellon Foundation, U.S. Agency for International Development, Smithsonian Institution; in Ecuador, Fundación Jatun Sacha, Estación Cientfica Yasuni de la Pontificia Universidad Católica del Ecuador, Estación de Biodiversidad Tiputini; in Peru, Natural Environment Research Council, National Geographic Society, National Science Foundation, WWF-U.S./Garden Club of America, Conservation International, MacArthur Foundation, Andrew W. Mellon Foundation, ACEER, Albergue Cuzco Amazonico, Explorama Tours S.A., Explorers Inn, IIAP, INRENA, UNAP and UNSAAC. Yadvinder Malhi gratefully acknowledges the generous support of a Royal Society University Research Fellowship.

## References

Achard F, Eva HD, Mayaux P *et al*. (2004) Improved estimates of net carbon emissions from land cover change in the tropics for the 1990s. *Global Biogeochemical Cycles*, **18**: art. no.-GB2008.

Achard F, Eva HD, Stibig HJ *et al*. (2002) Determination of deforestation rates of the world's humid tropical forests. *Science*, **297**, 999–1002.

van Andel T (2001) Floristic composition and diversity of mixed primary and secondary forest in northwest Guyana. *Biodiversity And Conservation*, **10**, 1645–1682.

Baker TR, Honorio E, Phillips OL *et al*. (submitted) Low stocks and rapid fluxes of coarse woody debris in southwestern Amazon forests. *Oecologia*.

Baker TR, Phillips OL, Malhi Y *et al*. (2004a) Increasing biomass in Amazonian forest plots. *Philosophical Transactions of the Royal Society of London Series B - Biological Sciences*, **359**, 353–365.

Baker TR, Phillips OL, Malhi Y *et al*. (2004b) Variation in wood density determines spatial patterns in Amazonian forest biomass. *Global Change Biology*, **10**, 545–562.

Balee W, Campbell DG (1990) Evidence for the successional status of liana forest (Xingu river basin, Amazonian Brazil). *Biotropica*, **22**, 36–47.

Brown S, Gaston G (1995) Use of forest inventories and geographic information systems to estimate biomass density of tropical forests: application to tropical Africa. *Environmental Monitoring and Assessment*, **38**, 157–168.

Brown S, Lugo AE (1992) Aboveground biomass estimates for Tropical Moist Forests of the Brazilian Amazon. *Interciencia*, **17**, 8–18.

Brown IF, Martineli LA, Thomas WW *et al*. (1995) Uncertainty in the biomass of Amazonian forests – an example from Rondonia, Brazil. *Forest Ecology And Management*, **75**, 175–189.

Campbell DG, Daly DC, Prance GT *et al*. (1986) Quantitative ecological inventory of terra firme and varzea tropical forest on the Rio Xingu, Brazilian Amazon. *Brittonia*, 369–393.

Castellanos HG (1998) Floristic composition and structure, tree diversity, and the relationship between floristic distribution and soil factors in El Caura Forest Reserve, southern Venezuela. In: *Forest biodiversity in North, Central and South America, and the Caribbean. Research and Monitoring*. MAB Series Vol. 21 (eds Dallmeier F, Comiskey JA), pp. 507–533. UNESCO, Paris.

Chave J, Brown ACS, Cairns MA *et al*. (2005) Tree allometry and improved estimation of carbon stocks and balance in tropical forests, *Oecologia*, **145**, 87–99.

Chave J, Condit R, Aguilar S *et al*. (2004) Error propagation and scaling for tropical forest biomass estimates. *Philosophical Transactions of the Royal Society of London Series B-Biological Sciences*, **359**, 409–420.

Chave J, Condit R, Lao S *et al*. (2003) Spatial and temporal variation of biomass in a tropical forest: results from a large census plot in Panama. *Journal of Ecology*, **91**, 240–252.

Chave J, Riera B, Dubois MA (2001) Estimation of biomass in a neotropical forest of French Guiana: spatial and temporal variability. *Journal Of Tropical Ecology*, **17**, 79–96.

Comiskey JA, Aymard G, Dallmeier F (1994) Structure and composition of lowland mixed forest in the Kwakwani region of Guyana. *Biottonia*, **10**, 13–28.

Comiskey JA, Campbell P, Alonso A *et al*. (2001) Vegetation assessment of the lower urubamba region, Peru. In: *Biodiversity of the Lower Urubamba Region, Peru*. SIMAB Series 7, (eds Dallmeier F, Alonso A, Campbell P), Smithsonian Inistitution/MAB Biodiversity Program, Washington, DC.

DeFries RS, Houghton RA, Hansen MC *et al*. (2002) Carbon emissions from tropical deforestation and regrowth based on satellite observations for the 1980s and 1990s. *Proceedings of the National Academy of Sciences of the United States of America*, **99**, 14256–14261.

DeWalt SJ, Chave J (2004) Structure and biomass of four lowland Neotropical forests. *Biotropica*, **36**, 7–19.

DNPM (1973–1983) Projeto RADAMBRASIL: Levantamento de Recursos Naturais, Vols 1–23 Rio de Janeiro, Miniserio das Minas e Energia, Departamento Nacional de Producao Mineral.

Eva HD, Belward AS, De Miranda EE *et al*. (2004) A land cover map of South America. *Global Change Biology*, **10**, 731–744.

FAO (2001) Global Forest Resources Assessment. FAO Forestry Paper 140.

Fearnside PM (1997) Greenhouse gases from deforestation in Brazilian Amazonia: Net committed emissions. *Climatic Change*, **35**, 321–360.

Ferreira LV, Prance GT (1998) Species richness and floristic composition four hectares in the Jaú National Park in upland forests in Central Amazonia. *Biodiversity and Conservation*, **7**, 1349–1364.

Groombridge B, Jenkins MD (2003) *World Atlas of Biodiversity*. University of California Press, Berkeley, California, USA.

Houghton RA, Lawrence KT, Hackler JL *et al*. (2001) The spatial distribution of forest biomass in the Brazilian Amazon: a comparison of estimates. *Global Change Biology*, **7**, 731–746.

Johnston M, Gillman M (1995) Tree population studies in low-diversity forests, Guyana. I. Floristic composition and stand structure. *Biodiversity and Conservation*, **4**, 339–362.

Keller M, Palace M, Asner GP *et al*. (2004) Coarse woody debris in undisturbed and logged forests in the eastern Brazilian Amazon. *Global Change Biology*, **10**, 784–795.

Keller M, Palace M, Hurtt G (2001) Biomass estimation in the Tapajos National Forest, Brazil – examination of sampling and allometric uncertainties. *Forest Ecology and Management*, **154**, 371–382.

Korning J, Balslev H (1994) Growth and mortality of trees in Amazonian tropical rain forest in Ecuador. *Journal of Vegetation Science*, **4**, 77–86.

Laurance WF, Fearnside PM, Laurance SG *et al*. (1999) Relationship between soils and Amazon forest biomass: a landscape-scale study. *Forest Ecology and Management*, **118**, 127–138.

Laurance WF, Laurance SG, Ferreira LV *et al*. (1997) Biomass collapse in Amazonian forest fragments. *Science*, **278**, 1117–1118.

Laurance WF, Oliveira AA, Laurance SG *et al*. (2004) Pervasive alteration of tree communities in undisturbed Amazonian forests. *Nature*, **428**, 171–175.

Lewis SL, Malhi Y, Phillips OL (2004) Fingerprinting the impacts of global change on tropical forests. *Philosophical Transactions of the Royal Society of London Series B - Biological Sciences*, **359**, 437–462.

Malhi Y, Baker TR, Phillips OL *et al*. (2004) The above-ground coarse wood productivity of 104 Neotropical forest plots. *Global Change Biology*, **10**, 563–591.

Malhi Y, Grace J (2000) Tropical forests and atmospheric carbon dioxide. *Trends in Ecology and Evolution*, **15**, 332–337.

Malhi Y, Phillips OL, Lloyd J *et al*. (2002) An international network to monitor the structure, composition and dynamics of Amazonian forests (RAINFOR). *Journal of Vegetation Science*, **13**, 439–450.

Malhi Y, Wood D, Baker TA *et al*. The productivity and carbon turnover of Amazon forest biomass, in preparation.

Meinzer FC, Andrade JL, Goldstein G *et al*. (1999) Partitioning of soil water among canopy trees in a seasonally dry tropical forest. *Oecologia*, **121**, 293–301.

Meinzer FC, Clearwater MJ, Goldstein G (2001) Water transport in trees: current perspectives, new insights and some controversies. *Environmental and Experimental Botany*, **45**, 239–262.

Milliken W (1998) Structure and composition of one hectare of central Amazonian terra firme forest. *Biotropica*, **30**, 530–537.

Mori SA, Rabelo BV, Tsou C-H *et al*. (1989) Composition and structure of an eastern Amazonian forest at Camaipi, Amapá, Brazil. *Bol. Mus. Paraense Hist. Nat.*, **5**, 3–18.

Nebel G, Kvist LP, Vanclay JK *et al*. (2001) Structure and floristic composition of flood plain forests in the Peruvian Amazon. I Overstorey. *Forest Ecology and Management*, **150**, 27–57.

Nepstad DC, Verissimo A, Alencar A *et al*. (1999) Large-scale impoverishment of Amazonian forests by logging and fire. *Nature*, **398**, 505–508.

Olson JS, Watts JA, Allison L (1983) *Carbon in Live Vegetation of Major World Ecosystems*. US Department of Energy, Washington, DC.

Peres CA (1994) Composition, density, and fruiting phenology of arborescent palms in an Amazonian terra-firme forest. *Biotropca*, **26**, 285–294.

Phillips OL, Baker TR, Arroyo L *et al*. (2004) Pattern and process in Amazon tree turnover, 1976–2001. *Philosophical Transactions of the Royal Society of London Series B - Biological Sciences*, **359**, 381–407.

Phillips OL, Gentry AH (1994) Increasing turnover through time in Tropical Forests. *Science*, **263**, 954–958.

Phillips OL, Malhi Y, Higuchi N *et al*. (1998) Changes in the carbon balance of tropical forests: evidence from long-term plots. *Science*, **282**, 439–442.

Phillips OL, Martinez RV, Arroyo L *et al*. (2002) Increasing dominance of large lianas in Amazonian forests. *Nature*, **418**, 770–774.

Pires JM, Salomão RP (2000) Dinâmica da diversidade arbórea de um fragmento de floresta tropical primária na Amazônia oriental – 1. Período: 1956 a 1992. *Boletim do Museu Paraense Emília Goeldi, Série Botanica*, **16**, 63–110.

Pitman NCA, Terborgh JW, Silman MR *et al*. (2001) Dominance and distribution of tree species in upper Amazonian terra firme forests. *Ecology*, **82**, 2101–2117.

Potter C, Genovese VB, Klooster S *et al*. (2001) Biomass burning losses of carbon estimated from ecosystem modeling and satellite data analysis for the Brazilian Amazon region. *Atmospheric Environment*, **35**, 1773–1781.

Potter CS (1999) Terrestrial biomass and the effects of deforestation on the global carbon cycle – results from a model of primary production using satellite observations. *Bioscience*, **49**, 769–778.

Prance GT, Rodrigues WA, da Silva MF (1976) Inventario florestal de um hectare de mata de terra firma, Km 30 da Estrada Manaus-Itacoatiara. *Acta Amazonica*, **6**, 9–35.

Rice AH, Pyle EH, Saleska SR *et al*. (2004) Carbon balance and vegetation dynamics in an old-growth Amazonian forest. *Ecological Applications*, **14**, S55–S71.

Roy R, Saugier B, Mooney HA (2001) *Terrestrial Global Productivity*. Academic Press, San Diego.

Salomão RP, Silva MFF, Lisboa PL (1988) Inventario ecológico em floresta pluvial tropical de terra firme, Serra Norte, Carajás, Pará. *Boletim do Museu Paraense Emílio Goeldi Serie Botânica*, 1–46.

Schimel D, Potter C (1995) Process modelling and spatial extrapolation. In: *Biogenic Trace Gases: Exchange Between Soils, Sediments, Aquatic Systems and the Atmosphere* (eds Matson PA, Harriss RC), Blackwell Science, Oxford.

de Silva ALL, Lisboa PLB, Maciel UN (1992) Diversidade florística e estructura em floresta densa da bacia do Rio Juruá-AM. Boletim do Museu Paraense Emílio Goeldi. *Botânica*, **8**, 203–258.

Silva MFF, Rosa NA, Oliveira J (1987) Estudos botânicos na área do projecto Ferro Carajás. 5. Aspectos florísticos da mata do Rio Gelado, Pará. *Boletim do Museu Paraense Emilio Goeldi. Serie Botânica*, **3**, 1–20.

Silva MFF, Rosa NA, Salomão RP (1986) Estudos botanicos na área do projecto Ferro Carajás. 3. Aspectos florísticos da mata do aeroporto de Serra Norte – PA. *Boletim do Museu Paraense Emilio Goeldi. Serie Botanica*, **2**, 169–187.

Smith DN, Killeen TJ (1998) A comparison of the structure and composition of montane and lowland tropical forest in the Serrania Pilón, Beni, Bolivia. In: *Forest biodiversity in North, Central and South America, and the Caribbean. Research and monitoring*. MAB Series Vol. 21 (eds Dallmeier F, Comiskey JA), pp. 681–700. UNESCO, Paris.

Sombroek W (2000) Amazon landforms and soils in relation to biological diversity. *Acta Amazonica*, **30**, 81–100.

Spichiger R, Loizeau P-A, Latour C *et al*. (1996) Tree species richness of a South-western Amazonian forest (Jenaro Herrera, Peru, 73°40′W/ 4°54′S). *Candollea*, **51**, 559–577.

Terborgh J, Andresen E (1998) The composition of Amazonian forests: patterns at local and regional scales. *Journal of Tropical Ecology*, **14**, 645–664.

Uhl C, Mvuphy PG (1981) Composition, structure, and regeneration of tierra firme forest in the Amazon basin of Venezuela. *Tropical Biology*, **22**, 219–237.

Veillon JP (1985) El crecimiento de algunos bosques naturales de Venezuela en relación con los parametros del medio ambiente. *Revista Forestel Venezolana*, **29**, 5–119.

de Walt SJ, Bourdy G, Chavez de Michel LR *et al*. (1999) Ethnobotany of the Tacana. Quantitative inventories of two permanent plots of northwestern Bolivia. *Economic Botany*, **53**, 237–260.

 

**Table A1** Metadata for the 227 forest plots used in this analysis

| Plot Name | Plot Code | | Country | Latitude (decimal) | Longitude (decimal) | Elevation (m) | Forest Type | Plot Size (ha) | Basal area ($m^2 ha^{-1}$) | Biomass$^+$ (Mg DW $ha^{-1}$) | Mean number of months <100 mm of rainfall | Mean monthly rainfall (mm) | Mean monthly temperature (°C) | Mean monthly solar ($MJ m^{-2} day^{-1}$) | ENSO-rainfall correlation |
|---|---|---|---|---|---|---|---|---|---|---|---|---|---|---|---|
| Amazonic | AMA-01 | Arroyo, Killeen (unpublished data) | Bolivia | −16.63 | −61.92 | 500 | Terra firme | 6.25 | 18.00 | 186.74/180.59 | 7.67 | 1052 | 24.83 | 18.63 | 0.015 |
| Amboro Rio Saguayo | AMB-01[1,2,3] | Smith & Killeen (1998) | Bolivia | −17.75 | −63.73 | 680* | Terra firme | 1 | 39.20 | 404.54/357.5 | 8.64 | 918 | 21.00 | 18.88 | 0.011 |
| BosqueChimanes: Aguas Negras | BCA-01 | Arroyo, Killeen (unpublished data) | Bolivia | −15.07 | −66.55 | 200 | Terra firme | 6 | 23.90 | 244.34/234.57 | 5.13 | 1713 | 25.45 | 18.71 | −0.048 |
| BosqueChimanes: Chirizi | BCC-01 | Arroyo, Killeen (unpublished data) | Bolivia | −15.58 | −66.17 | 200 | Terra firme | 10 | 22.86 | 234.09/224.37 | 4.51 | 1850 | 25.31 | 18.79 | −0.035 |
| BosqueChimanes: Jamanchi | BCJ-01 | Arroyo, Killeen (unpublished data) | Bolivia | −15.28 | −66.47 | 200 | Terra firme | 10 | 28.45 | 291.02/289.78 | 4.82 | 1790 | 25.91 | 18.61 | −0.037 |
| BosqueChimanes: Infierno Verde | BCV-01 | Arroyo, Killeen (unpublished data) | Bolivia | −15 | −66 | 200 | Terra firme | 1 | 25.70 | 263.11/252.24 | 4.41 | 1857 | 26.04 | 18.55 | −0.024 |
| Beni 1 | BEN-01 | Comiskey *et al.* (2000) | Bolivia | −14.78 | −66.34 | 200* | Seasonally flooded | 1 | 30.85 | 315.48/298.49 | 5.03 | 1713 | 26.26 | 18.45 | −0.025 |
| Beni 2 | BEN-02 | Comiskey *et al.* (2000) | Bolivia | −14.77 | −66.35 | 200* | Terra firme | 1 | 31.00 | 316.98/299.94 | 5.03 | 1713 | 26.26 | 18.45 | −0.025 |
| Beni 10 | BEN-10[1,2,3] | Comiskey *et al.* (2000) | Bolivia | −14.89 | −66.59 | 250* | Terra firme | 1 | 42.38 | 433.15/410.05 | 5.23 | 1709 | 26.15 | 18.50 | −0.031 |
| Beni 12 | BEN-12 | Comiskey *et al.* (2000) | Bolivia | −14.7 | −66.12 | 200* | Terra firme | 1 | 26.10 | 267.04/252.53 | 5.03 | 1713 | 26.26 | 18.45 | −0.025 |
| Beni 14 | BEN-14 | Comiskey *et al.* (2000) | Bolivia | −14.74 | −66.56 | 200* | Terra firme | 1 | 31.52 | 322.49/304.97 | 5.23 | 1709 | 26.15 | 18.50 | −0.031 |
| Beni 5 | BEN-5[1,2] | Comiskey *et al.* (2000) | Bolivia | −14.75 | −66.37 | 200* | Terra firme | 1 | 39.45 | 403.38/381.7 | 5.03 | 1713 | 26.26 | 18.45 | −0.025 |
| Beni 9 | BEN-9[1,2] | Comiskey *et al.* (2000) | Bolivia | −14.73 | −66.32 | 200* | Terra firme | 1 | 39.37 | 402.61/380.92 | 5.03 | 1713 | 26.26 | 18.45 | −0.025 |
| La Chonta | CHN-01 | RAINFOR (unpublished data) | Bolivia | −16.7 | −62 | 275* | Terra firme | 4 | 32.28 | 334.8/323.87 | 7.67 | 1052 | 24.83 | 18.63 | 0.015 |
| Chore 1 | CHO-01 | RAINFOR (unpublished data) | Bolivia | −14.35 | −61.16 | 170 | Terra firme | 1 | 14.51 | **131.23** | 6.23 | 1357 | 25.88 | 17.64 | 0.001 |
| Chore 2 | CHO-02 | Arroyo, Killeen (unpublished data) | Bolivia | −14.35 | −61.16 | 170 | Terra firme | 1 | 11.99 | 125.1/123.78 | 6.23 | 1357 | 25.88 | 17.64 | 0.001 |
| Cerro Pelao 1 | CRP-01 | RAINFOR (unpublished data) | Bolivia | −14.54 | −61.48 | 350 | Terra firme | 1 | 19.91 | **215.39** | 6.49 | 1297 | 25.73 | 17.85 | 0.044 |
| Cerro Pelao 2 | CRP-02 | RAINFOR (unpublished data) | Bolivia | −14.53 | −61.48 | 350 | Terra firme | 1 | 24.78 | **234.03** | 6.49 | 1297 | 25.73 | 17.85 | 0.044 |
| Huanchaca Uno 1 plot 1 | HCC-11 | Arroyo, Killeen (unpublished data) | Bolivia | −13.9 | −60.8 | 550 | Terra firme | 1 | 31.07 | **258.84** | 5.77 | 1454 | 25.58 | 17.33 | 0.009 |
| Huanchaca Uno 1 plot 2 | HCC-12 | Arroyo, Killeen (unpublished data) | Bolivia | −13.9 | −60.8 | 550 | Terra firme | 1 | 31.25 | **284.8** | 5.77 | 1454 | 25.58 | 17.33 | 0.009 |
| Los Fierros Bosque I | LFB-01 | RAINFOR (unpublished data) | Bolivia | −14.61 | −60.87 | 225 | Terra firme | 1 | 24.99 | **245.81** | 6.46 | 1313 | 25.12 | 17.69 | 0.011 |

Table A1. (Contd.)

| Plot Name | Plot Code | | Country | Latitude (decimal) | Longitude (decimal) | Elevation (m) | Forest Type | Plot Size (ha) | Basal area ($m^2 ha^{-1}$) | Biomass$^+$ (Mg DW $ha^{-1}$) | Mean number of months <100 mm of rainfall | Mean monthly rainfall (mm) | Mean monthly temperature (°C) | Mean monthly solar (MJ $m^{-2}$ $day^{-1}$) | ENSO-rainfall correlation |
|---|---|---|---|---|---|---|---|---|---|---|---|---|---|---|---|
| Los Fierros Bosque II | LFB-02 | RAINFOR (unpublished data) | Bolivia | −14.6 | −60.85 | 225 | Terra firme | 1 | 29.00 | **291.37** | 6.46 | 1313 | 25.12 | 17.69 | 0.011 |
| Lomerio | LOM-01 | Arroyo, Killeen (unpublished data) | Bolivia | −16.63 | −61.92 | 500 | Terra firme | 22.5 | 23.27 | 241.42/233.47 | 7.67 | 1052 | 24.83 | 18.63 | 0.015 |
| Las Londras plot 1 | LSL-01 | RAINFOR (unpublished data) | Bolivia | −14.4 | −61.13 | 170 | Seasonally flooded | 1 | 18.01 | **177.17** | 6.23 | 1357 | 25.88 | 17.64 | 0.001 |
| Las Londras plot 2 | LSL-02 | RAINFOR (unpublished data) | Bolivia | −14.4 | −61.13 | 170 | Seasonally flooded | 1 | 22.98 | **205.68** | 6.23 | 1357 | 25.88 | 17.64 | 0.001 |
| NK: Acuario 1 | NKA-01 | Arroyo, Killeen (unpublished data) | Bolivia | −15.25 | −61.24 | 300 | Terra firme | 1 | 19.20 | 199.83/199.91 | 6.72 | 1227 | 25.31 | 18.01 | 0.045 |
| NK: Acuario 2 | NKA-02 | Arroyo, Killeen (unpublished data) | Bolivia | −15.25 | −61.24 | 300 | Terra firme | 1 | 19.10 | 198.79/198.87 | 6.72 | 1227 | 25.31 | 18.01 | 0.045 |
| NK: Bosque Continuo 1 | NKC-01 | Arroyo, Killeen (unpublished data) | Bolivia | −14.3 | −60.53 | 800 | Terra firme | 1 | 26.76 | 279.35/270.23 | 6.08 | 1367 | 25.10 | 17.52 | 0.016 |
| NK: Bosque Continuo 2 | NKC-02 | Arroyo, Killeen (unpublished data) | Bolivia | −14.3 | −60.53 | 800 | Terra firme | 1 | 23.60 | 246.36/238.32 | 6.08 | 1367 | 25.10 | 17.52 | 0.016 |
| NoelKempff: Enano 1 | NKE-01 | Arroyo, Killeen (unpublished data) | Bolivia | −13.64 | −60.89 | 520 | Terra firme | 1 | 14.26 | 148.96/147.21 | 5.77 | 1454 | 25.58 | 17.33 | 0.009 |
| NoelKempff: Enano 2 | NKE-02[3] | Arroyo, Killeen (unpublished data) | Bolivia | −13.64 | −60.89 | 520 | Terra firme | 1 | 13.95 | 145.72/144.01 | 5.77 | 1454 | 25.58 | 17.33 | 0.009 |
| NoelKempff: Las Gamas | NKG-01[1,2] | Arroyo, Killeen (unpublished data) | Bolivia | −14.8 | −60.39 | 850 | Terra firme | 1 | 34.27 | 357.44/345.78 | 6.44 | 1332 | 24.64 | 17.51 | −0.008 |
| NoelKempff: Isla 1 | NKI-01 | Arroyo, Killeen (unpublished data) | Bolivia | −14.56 | −60.75 | 700 | Terra firme | 1 | 28.32 | 295.38/285.75 | 6.46 | 1313 | 25.12 | 17.69 | 0.011 |
| NoelKempff: Isla 2 | NKI-02 | Arroyo, Killeen (unpublished data) | Bolivia | −14.57 | −60.74 | 800 | Terra firme | 1 | 25.48 | 265.76/257.09 | 6.46 | 1313 | 25.12 | 17.69 | 0.011 |
| NoelKempff: Monte Cristo 1 | NKM-01[1,2,3] | Arroyo, Killeen (unpublished data) | Bolivia | −14.64 | −61.16 | 200 | Seasonally flooded | 1 | 34.46 | 359.21/355.75 | 6.49 | 1297 | 25.73 | 17.85 | 0.044 |
| NoelKempff: Monte Cristo 2 | NKM-02 | Arroyo, Killeen (unpublished data) | Bolivia | −14.71 | −61.15 | 200 | Seasonally flooded | 1 | 27.93 | 291.09/288.34 | 6.49 | 1297 | 25.73 | 17.85 | 0.044 |
| NoelKempff: Las Torres 1 | NKT-01[1,2,3] | Arroyo, Killeen (unpublished data) | Bolivia | −13.65 | −60.83 | 200 | Terra firme | 1 | 9.88 | 103.21/102 | 5.77 | 1454 | 25.58 | 17.33 | 0.009 |
| NoelKempff: Las Torres 2 | NKT-02[1,2,3] | Arroyo, Killeen (unpublished data) | Bolivia | −13.65 | −60.83 | 200 | Terra firme | 1 | 10.96 | 114.5/113.15 | 5.77 | 1454 | 25.58 | 17.33 | 0.009 |
| NoelKempff: Monte Verde | NKV-01 | Arroyo, Killeen (unpublished data) | Bolivia | −15.01 | −61.13 | 200 | Terra firme | 1 | 21.75 | 226.42/226.42 | 6.72 | 1227 | 25.31 | 18.01 | 0.045 |

Table A1. (Contd.)

| Plot Name | Plot Code | | Country | Latitude (decimal) | Longitude (decimal) | Elevation (m) | Forest Type | Plot Size (ha) | Basal area ($m^2 ha^{-1}$) | Biomass⁺ (Mg DW $ha^{-1}$) | Mean number of months <100 mm of rainfall | Mean monthly rainfall (mm) | Mean monthly temperature (°C) | Mean monthly solar ($MJ m^{-2} day^{-1}$) | ENSO-rainfall correlation |
|---|---|---|---|---|---|---|---|---|---|---|---|---|---|---|---|
| Perseverancia | PER-01 | Smith & Killeen (1998) | Bolivia | −14.55 | −62.75 | 250* | Terra firme | 1 | 23.38 | 242.47/241.36 | 6.67 | 1273 | 25.80 | 18.17 | 0.019 |
| Pilon Lajas: Rio Colorado | PIL-01 | Smith & Killeen (1998) | Bolivia | −14.92 | −67.08 | 270 | Terra firme | 1 | 26.40 | 269.49/242.87 | 4.87 | 1730 | 25.27 | 18.58 | −0.033 |
| Pilon Lajas: Cumbre Pilon | PIL-02 | Smith & Killeen (1998) | Bolivia | −15.25 | −67 | 900 | Terra firme | 1 | 30.62 | 312.77/311.96 | 5.13 | 1713 | 25.45 | 18.71 | −0.048 |
| Tacana | TAC-01 | DeWalt *et al.* (1999) | Bolivia | −13.67 | −68.2 | 250 | Terra firme | 1 | 24.96 | 253.56/229.62 | 3.74 | 2052 | 24.40 | 18.34 | 0.008 |
| Taruma | TAR-01 | Arroyo, Killeen (unpublished data) | Bolivia | −13.97 | −61.65 | 225 | Terra firme | 8 | 20.23 | 210.73/208.84 | 5.92 | 1383 | 25.91 | 17.56 | −0.011 |
| Balee 1: P.I. Guaja/R. Turiacu | BAL-01 | Balee (1990) | Brazil | −3.1 | −45.97 | 90* | Terra firme | 1 | 27.20 | 293.96/292.6 | 5.64 | 1950 | 26.85 | 16.31 | −0.218 |
| Balee 2: Urutawi/ (Turicau basin) | BAL-02 | Balee (1990) | Brazil | −3.1 | −45.97 | 90* | Terra firme | 1 | 25.30 | 273.42/272.16 | 5.64 | 1950 | 26.85 | 16.31 | −0.218 |
| Balee 3: Gurupiuna (Gurupi basin) | BAL-03 | Balee (1990) | Brazil | −2.67 | −46.33 | 100* | Terra firme | 1 | 30.30 | 327.54/333.64 | 5.08 | 2104 | 26.39 | 16.20 | −0.221 |
| Balee 4: P.I. Caninde/R. Gurupi | BAL-04[1,3] | Balee (1990) | Brazil | −2.67 | −46.33 | 100* | Terra firme | 1 | 34.50 | 372.95/379.88 | 5.08 | 2104 | 26.39 | 16.20 | −0.221 |
| BDFFP 2303 Faz. Dimona 4–6 | BDF-01 | Laurance *et al.* (1999) | Brazil | −2.4 | −60 | 75 | Terra firme | 2 | 30.25 | **380.88** | 3.05 | 2167 | 27.00 | 15.28 | −0.260 |
| BDFFP 2303 Faz. Dimona 7–9 | BDF-02 | Laurance *et al.* (1999) | Brazil | −2.4 | −60 | 75 | Terra firme | 3 | 29.40 | 325.62/322.88 | 3.05 | 2167 | 27.00 | 15.28 | −0.260 |
| BDFFP 1101 Gaviao | BDF-03 | Laurance *et al.* (1999) | Brazil | −2.4 | −59.9 | 75 | Terra firme | 1 | 29.51 | **339.64** | 3.05 | 2167 | 27.00 | 15.28 | −0.260 |
| BDFFP 1102 Gaviao | BDF-04[1,2,3] | Laurance *et al.* (1999) | Brazil | −2.4 | −59.9 | 75 | Terra firme | 1 | 22.51 | **250.9** | 3.05 | 2167 | 27.00 | 15.28 | −0.260 |
| BDFFP 1103 Gaviao | BDF-05 | Laurance *et al.* (1999) | Brazil | −2.4 | −59.9 | 75 | Terra firme | 1 | 25.67 | **306.98** | 3.05 | 2167 | 27.00 | 15.28 | −0.260 |
| BDFFP 1201 Gaviao | BDF-06 | Laurance *et al.* (1999) | Brazil | −2.4 | −59.9 | 75 | Terra firme | 3 | 25.97 | **300.59** | 3.05 | 2167 | 27.00 | 15.28 | −0.260 |
| BDFFP 1105 Gaviao | BDF-07 | Laurance *et al.* (1999) | Brazil | −2.4 | −59.9 | 75 | Terra firme | 1 | 28.21 | 312.42/309.81 | 3.05 | 2167 | 27.00 | 15.28 | −0.260 |
| BDFFP 1109 Gaviao | BDF-08 | Laurance *et al.* (1999) | Brazil | −2.4 | −59.9 | 75 | Terra firme | 1 | 28.09 | **322.24** | 3.05 | 2167 | 27.00 | 15.28 | −0.260 |
| BDFFP 1113 Florestal | BDF-09 | Laurance *et al.* (1999) | Brazil | −2.4 | −59.9 | 75 | Terra firme | 1 | 29.81 | 330.14/327.38 | 3.05 | 2167 | 27.00 | 15.28 | −0.260 |

Table A1. (Contd.)

| Plot Name | Plot Code | | Country | Latitude (decimal) | Longitude (decimal) | Elevation (m) | Forest Type | Plot Size (ha) | Basal area ($m^2 ha^{-1}$) | Biomass[+] (Mg DW $ha^{-1}$) | Mean number of months <100 mm of rainfall | Mean monthly rainfall (mm) | Mean monthly temperature (°C) | Mean monthly solar ($MJ m^{-2} day^{-1}$) | ENSO-rainfall correlation |
|---|---|---|---|---|---|---|---|---|---|---|---|---|---|---|---|
| BDFFP 1301 Florestal 1 = plot 1301.1 | BDF-10 | Laurance *et al*, (1999) | Brazil | −2.4 | −59.9 | 75 | Terra firme | 1 | 28.30 | **330.45** | 3.05 | 2167 | 27.00 | 15.28 | −0.260 |
| BDFFP 1301 Florestal 2 = plots 1301.456 | BDF-11 | Laurance *et al*. (1999) | Brazil | −2.4 | −59.9 | 75 | Terra firme | 3 | 30.27 | **357.97** | 3.05 | 2167 | 27.00 | 15.28 | −0.260 |
| BDFFP 1301 Florestal 3 = plots 1301.78 | BDF-12 | Laurance *et al*. (1999) | Brazil | −2.4 | −59.9 | 75 | Terra firme | 2 | 29.40 | **351.74** | 3.05 | 2167 | 27.00 | 15.28 | −0.260 |
| BDFFP 3402 Cabo Frio | BDF-13 | Laurance *et al*. (1999) | Brazil | −2.4 | −60 | 75 | Terra firme | 9 | 28.53 | **344.35** | 3.05 | 2167 | 27.00 | 15.28 | −0.260 |
| BDFFP 3304 Porto Alegre | BDF-14 | Laurance *et al*. (1999) | Brazil | −2.4 | −60 | 75 | Terra firme | 2 | 30.69 | **358.69** | 3.05 | 2167 | 27.00 | 15.28 | −0.260 |
| Bionte 1 | BNT-01 | Higuchi *et al*. (unpublished data) | Brazil | −2.63 | −60.17 | 70* | Terra firme | 1 | 31.15 | 345.02/342.13 | 3.00 | 2272 | 27.23 | 15.20 | −0.227 |
| Bionte 2 | BNT-02 | Higuchi *et al*. (unpublished data) | Brazil | −2.63 | −60.17 | 70* | Terra firme | 1 | 33.04 | 365.86/362.8 | 3.00 | 2272 | 27.23 | 15.20 | −0.227 |
| Bionte 4 | BNT-04 | Higuchi *et al*. (unpublished data) | Brazil | −2.63 | −60.17 | 70* | Terra firme | 1 | 28.98 | 320.97/318.28 | 3.00 | 2272 | 27.23 | 15.20 | −0.227 |
| Bionte T4 B2 SB1 | BNT-05 | Higuchi *et al*. (unpublished data) | Brazil | −2.63 | −60.17 | 70* | Terra firme | 1 | 27.28 | 302.09/299.56 | 3.00 | 2272 | 27.23 | 15.20 | −0.227 |
| Bionte T4 B1 SB3 | BNT-06 | Higuchi *et al*. (unpublished data) | Brazil | −2.63 | −60.17 | 70* | Terra firme | 1 | 30.85 | 341.61/338.75 | 3.00 | 2272 | 27.23 | 15.20 | −0.227 |
| Bionte T4 B4 SB4 | BNT-07 | Higuchi *et al*. (unpublished data) | Brazil | −2.63 | −60.17 | 70* | Terra firme | 1 | 31.39 | 347.59/344.68 | 3.00 | 2272 | 27.23 | 15.20 | −0.227 |
| BR-364 km17 P.M. – J. Rondônia | BRR-01 | Thomsen PhD thesis | Brazil | −10.75 | −61.92 | 190* | Terra firme | 1 | 31.05 | 326.65/305.53 | 4.64 | 1826 | 25.70 | 16.35 | −0.023 |
| Camaipi | CAI-01 | Mori *et al*. (1989) | Brazil | 0.17 | −51.62 | 30* | Terra firme | 1 | 35.10 | 382.71/386.44 | 4.79 | 1993 | 25.54 | 15.48 | −0.114 |
| Caxiuana 1 | CAX-01 | RAINFOR (unpublished data) | Brazil | −1.7 | −51.53 | 15 | Terra firme | 1 | 30.75 | **430.33** | 3.97 | 2314 | 26.96 | 15.71 | −0.206 |
| Caxiuana 2 | CAX-02 | Almeida *et al*. (unpublished data) | Brazil | −1.7 | −51.53 | 15 | Terra firme | 1 | 32.28 | **385.48** | 3.97 | 2314 | 26.96 | 15.71 | −0.206 |
| Caxiuana 3 | CAX-03 | Almeida *et al*. (unpublished data) | Brazil | −1.7 | −51.53 | 15 | Terra firme | 1 | 32.15 | 350.79/353.96 | 3.97 | 2314 | 26.96 | 15.71 | −0.206 |
| Caxiuana 4 | CAX-04 | Almeida *et al*. (unpublished data) | Brazil | −1.7 | −51.53 | 15 | Terra firme | 1 | 31.03 | 338.57/341.63 | 3.97 | 2314 | 26.96 | 15.71 | −0.206 |

Table A1. (Contd.)

| Plot Name | Plot Code | | Country | Latitude (decimal) | Longitude (decimal) | Elevation (m) | Forest Type | Plot Size (ha) | Basal area ($m^2 ha^{-1}$) | Biomass$^+$ (Mg DW $ha^{-1}$) | Mean number of months <100 mm of rainfall | Mean monthly rainfall (mm) | Mean monthly temperature (°C) | Mean monthly solar ($MJ m^{-2} day^{-1}$) | ENSO-rainfall correlation |
|---|---|---|---|---|---|---|---|---|---|---|---|---|---|---|---|
| Caxiuana 5 | CAX-05 | Almeida *et al.* (unpublished data) | Brazil | −1.7 | −51.53 | 15 | Terra firme | 1 | 30.53 | 333.12/336.13 | 3.97 | 2314 | 26.96 | 15.71 | −0.206 |
| Ducke | DUC-01 | Prance *et al.* (1976) | Brazil | −3 | −60 | 45* | Terra firme | 1 | 24.68 | 272.71/270.99 | 3.49 | 2247 | 27.23 | 15.13 | −0.224 |
| Fazenda Nova Olinda | FAZ-01 | Silveira *et al.* (unpublished data) | Brazil | −10.12 | −69.22 | 170* | Terra firme | 1 | 34.16 | 345.4/333.04 | 4.15 | 1998 | 25.78 | 16.62 | −0.022 |
| Jacaranda plots 1–5 | JAC-01 | Higuchi *et al.* (unpublished data) | Brazil | −2.63 | −60.17 | 75* | Terra firme | 5 | 27.25 | 301.84/299.31 | 3.00 | 2272 | 27.23 | 15.20 | −0.227 |
| Jacaranda plots 6–10 | JAC-02 | Higuchi *et al.* (unpublished data) | Brazil | −2.63 | −60.17 | 75* | Terra firme | 5 | 26.37 | 291.99/289.55 | 3.00 | 2272 | 27.23 | 15.20 | −0.227 |
| Jau 1 | JAU-01[1,2,3] | Ferreira & Prance (1998) | Brazil | −2.5 | −62 | 35* | Terra firme | 1 | 37.50 | 411.62/380.81 | 2.08 | 2303 | 27.02 | 15.20 | −0.210 |
| Jau 2 | JAU-02 | Ferreira & Prance (1998) | Brazil | −2.5 | −62 | 35* | Terra firme | 1 | 32.80 | 360.03/333.08 | 2.08 | 2303 | 27.02 | 15.20 | −0.210 |
| Jau 3 | JAU-03[1,2,3] | Ferreira & Prance (1998) | Brazil | −2.5 | −62 | 35* | Terra firme | 1 | 37.80 | 414.91/383.86 | 2.08 | 2303 | 27.02 | 15.20 | −0.210 |
| Jau 4 | JAU-04[1,2,3] | Ferreira & Prance (1998) | Brazil | −2.5 | −62 | 35* | Terra firme | 1 | 40.20 | 441.26/408.23 | 2.08 | 2303 | 27.02 | 15.20 | −0.210 |
| Jari 1 | JRI-01 | J.M.N. Silva, (unpublished data) | Brazil | −1 | −52.05 | 85* | Terra firme | 1 | 33.12 | **392.4** | 3.95 | 2346 | 26.94 | 15.82 | −0.240 |
| Juruá (Jaraqui) | JUR-01 | da Silva, Lisboa, Maciel (1992) | Brazil | −4.3 | −66.37 | 65* | Terra firme | 1 | 33.93 | 360.46/344.86 | 1.56 | 2518 | 26.62 | 15.17 | −0.146 |
| Juruá (Jurua-I)) | JUR-02 | da Silva, Lisboa, Maciel (1992) | Brazil | −4.78 | −66.25 | 80* | Terra firme | 1 | 27.02 | 286.43/274.64 | 2.13 | 2512 | 26.64 | 15.20 | −0.103 |
| Juruá (Munguba) | JUR-03 | da Silva, Lisboa, Maciel (1992) | Brazil | −4.95 | −66.58 | 80* | Terra firme | 1 | 30.73 | 324.89/312.36 | 2.15 | 2551 | 26.43 | 15.20 | −0.099 |
| Juruá (Nej-I) | JUR-04 | da Silva, Lisboa, Maciel (1992) | Brazil | −4.67 | −66.17 | 80* | Terra firme | 1 | 29.75 | 315.86/302.4 | 2.13 | 2512 | 26.64 | 15.20 | −0.103 |
| Mare | MAE-01 | Milliken (1998) | Brazil | −1.75 | −61.25 | 50* | Terra firme | 1 | 27.95 | 307.64/283.71 | 2.18 | 2272 | 26.97 | 15.31 | −0.237 |
| Marabá: UA1 | MAR-01 | Salomao *et al.* (unpublished data) | Brazil | −5.73 | −49.05 | 90 | Terra firme | 2 | 20.39 | 219.96/207.09 | 5.33 | 1956 | 26.64 | 15.83 | −0.173 |
| Marabá: UA2 | MAR-02 | Salomao *et al.* (unpublished data) | Brazil | −5.7 | −49.03 | 90 | Terra firme | 2 | 28.52 | 307.65/289.65 | 5.33 | 1956 | 26.64 | 15.83 | −0.173 |
| Marabá: UA3 | MAR-03[3] | Salomao *et al.* (unpublished data) | Brazil | −5.7 | −49 | 90 | Terra firme | 2 | 31.20 | 336.53/316.84 | 5.59 | 1850 | 26.51 | 15.98 | −0.181 |
| Mocambo | MBO-01 | Pires & Salamao (2000) | Brazil | −1.45 | −48.45 | 24 | Terra firme | 2 | 27.73 | 301.15/270.37 | 2.82 | 2933 | 26.67 | 16.15 | −0.133 |

Table A1. (Contd.)

| Plot Name | Plot Code | | Country | Latitude (decimal) | Longitude (decimal) | Elevation (m) | Forest Type | Plot Size (ha) | Basal area ($m^2 ha^{-1}$) | Biomass+ (Mg DW $ha^{-1}$) | Mean number of months <100 mm of rainfall | Mean monthly rainfall (mm) | Mean monthly temperature (°C) | Mean monthly solar ($MJ m^{-2} day^{-1}$) | ENSO-rainfall correlation |
|---|---|---|---|---|---|---|---|---|---|---|---|---|---|---|---|
| PARNA Serra do Divisor: Serra da Jaquirana | PAA-01[1,2,3] | Silveira *et al.* (unpublished data) | Brazil | −7.44 | −73.67 | 200* | Terra firme | 1 | 8.87 | 88.55/82.09 | 3.00 | 1953 | 26.42 | 15.39 | −0.073 |
| PARNA Serra do Divisor: Rio Azul | PAA-02 | Silveira *et al.* (unpublished data) | Brazil | −7.54 | −73.28 | 200* | Terra firme | 1 | 31.82 | 317.83/310.23 | 2.82 | 2028 | 26.47 | 15.48 | −0.098 |
| PARNA Serra do Divisor: Rio Branco | PAA-03 | Silveira *et al.* (unpublished data) | Brazil | −8.27 | −73.23 | 200* | Terra firme | 1 | 18.35 | 183.45/169.82 | 3.08 | 2048 | 26.41 | 15.61 | −0.085 |
| PARNA Serra do Divisor: Rio Juruá | PAA-05 | Silveira *et al.* (unpublished data) | Brazil | −8.56 | −72.88 | 200* | Terra firme | 1 | 24.15 | 241.62/245.24 | 2.74 | 2171 | 26.34 | 15.77 | −0.059 |
| Peixe-Boi | PEB-01 | Salomao *et al.* (unpublished data) | Brazil | −1 | −47.5 | 10* | Terra firme | 3 | 23.30 | 253.04/256.53 | 3.85 | 2553 | 26.34 | 16.05 | −0.205 |
| RESEX Alto Juruá: Seringal São João | RES-01 | Silveira *et al.* (unpublished data) | Brazil | −9.08 | −72.68 | 200* | Terra firme | 1 | 26.58 | 266.15/245.99 | 2.51 | 2227 | 25.91 | 15.99 | −0.074 |
| RESEX Alto Juruá: Seringal Restauração | RES-02 | Silveira *et al.* (unpublished data) | Brazil | −9.08 | −72.68 | 200* | Terra firme | 1 | 30.78 | 308.2/284.86 | 2.51 | 2227 | 25.91 | 15.99 | −0.074 |
| RESEX Chico Mendes: Seringal Porongaba 1 | RES-03 | Silveira *et al.* (unpublished data) | Brazil | −10.82 | −68.77 | 20* | Terra firme | 1 | 31.32 | 317.11/317.92 | 4.36 | 1904 | 25.82 | 16.87 | −0.015 |
| RESEX Chico Mendes: Seringal Porongaba 2 | RES-04 | Silveira *et al.* (unpublished data) | Brazil | −10.82 | −68.77 | 200* | Terra firme | 1 | 24.64 | 249.47/250.11 | 4.36 | 1904 | 25.82 | 16.87 | −0.015 |
| RESEX Chico Mendes: Seringal Dois Irmãos 1 | RES-05 | Silveira *et al.* (unpublished data) | Brazil | −10.57 | −68.32 | 200* | Terra firme | 1 | 31.06 | 314.87/315.41 | 4.46 | 1870 | 25.94 | 16.72 | −0.019 |
| RESEX Chico Mendes: Seringal Dois Irmãos 2 | RES-06[1,2,3] | Silveira *et al.* (unpublished data) | Brazil | −10.57 | −68.32 | 200* | Terra firme | 1 | 14.97 | 151.76/152.02 | 4.46 | 1870 | 25.94 | 16.72 | −0.019 |
| RO-429 km 90 | ROR-01 | Thomsen PhD thesis | Brazil | −11.33 | −63.5 | 375* | Terra firme | 1 | 26.07 | 271.38/240.55 | 5.15 | 1567 | 25.35 | 16.61 | −0.030 |
| RO-429 km 15 | ROR-02 | Thomsen PhD thesis | Brazil | −11 | −62.25 | 200* | Terra firme | 1 | 34.47 | 358.82/318.06 | 4.97 | 1697 | 25.79 | 16.53 | −0.022 |
| Sao Francisco do Para | SAF-01 | Vieira *et al.* (unpublished data) | Brazil | −1.07 | −47.78 | 10* | Terra firme | 1 | 26.26 | 285.18/289.12 | 3.46 | 2754 | 26.50 | 16.14 | −0.162 |
| Rondonia: Samuel Hydroelectric Reservoir | SAM-01 | Foster Brown *et al.* (1995) | Brazil | −8.75 | −63.38 | 110* | Terra firme | 1 | 25.10 | 264.55/254.51 | 3.90 | 2163 | 26.19 | 15.67 | 0.003 |

 

Table A1. (Contd.)

| Plot Name | Plot Code | | Country | Latitude (decimal) | Longitude (decimal) | Elevation (m) | Forest Type | Plot Size (ha) | Basal area ($m^2 ha^{-1}$) | Biomass+ (Mg DW $ha^{-1}$) | Mean number of months <100 mm of rainfall | Mean monthly rainfall (mm) | Mean monthly temperature (°C) | Mean monthly solar ($MJ m^{-2} day^{-1}$) | ENSO-rainfall correlation |
|---|---|---|---|---|---|---|---|---|---|---|---|---|---|---|---|
| Rio Gelado Serra Norte Carajás | SER-01 | da Silva, Rosa, Oliveira (1987) | Brazil | −6.33 | −50.25 | 500* | Terra firme | 1 | 17.54 | 189.4/185.41 | 4.85 | 1973 | 25.64 | 15.65 | −0.137 |
| Pojuca Itacaiúnas Serra Norte Carajás | SER-02 | da Silva, Rosa (1989), Thomsen Phd thesis | Brazil | −6 | −50.25 | 760* | Terra firme | 1 | 20.27 | 218.92/205.74 | 4.85 | 1973 | 25.64 | 15.65 | −0.137 |
| Three-Alpha Itacaiúnas Serra Norte Carajás | SER-03 | da Silva, Rosa (1989), Thomsen Phd thesis | Brazil | −6 | −50.25 | 760* | Terra firme | 1 | 22.66 | 244.73/230 | 4.85 | 1973 | 25.64 | 15.65 | −0.137 |
| Aeroporto Serra Norte Carajás | SER-04 | da Silva *et al.* (1986), Thomsen Phd thesis | Brazil | −6 | −50.25 | 760* | Terra firme | 1 | 27.72 | 299.38/281.36 | 4.85 | 1973 | 25.64 | 15.65 | −0.137 |
| Minas Serra Norte Carajás | SER-05 | Salomao, da Silva, Rosa (1988), Thomsen Phd | Brazil | −6 | −50.17 | 760* | Terra firme | 1 | 21.59 | 233.23/228.22 | 4.85 | 1973 | 25.64 | 15.65 | −0.137 |
| Tapajos RP014 1–4 | TAP-01 | J.M.N. Silva, (unpublished data) | Brazil | −2.75 | −55 | 20* | Terra firme | 1 | 26.89 | **300.06** | 4.51 | 1968 | 26.33 | 16.17 | −0.284 |
| Tapajos RP014 5–8 | TAP-02 | J.M.N. Silva, (unpublished data) | Brazil | −2.75 | −55 | 20* | Terra firme | 1 | 31.31 | **374.63** | 4.51 | 1968 | 26.33 | 16.17 | −0.284 |
| Tapajos RP014 9–12 | TAP-03 | J.M.N. Silva, (unpublished data) | Brazil | −2.75 | −55 | 20* | Terra firme | 1 | 34.39 | **375.9** | 4.51 | 1968 | 26.33 | 16.17 | −0.284 |
| Trombetas 1 | TRO-01 | Salomao *et al.* (unpublished data) | Brazil | −1.5 | −56.5 | 50* | Terra firme | 1 | 30.50 | 334.46/336.21 | 4.31 | 2023 | 27.08 | 15.98 | −0.353 |
| Trombetas 2 | TRO-02 | Salomao *et al.* (unpublished data) | Brazil | −1.5 | −56.5 | 50* | Terra firme | 1 | 22.10 | 242.35/243.62 | 4.31 | 2023 | 27.08 | 15.98 | −0.353 |
| Urucu | URU-01 | Peres (1994) | Brazil | −4.85 | −65.27 | 100* | Terra firme | 5 | 33.20 | 353.89/337.43 | 2.00 | 2419 | 26.71 | 15.23 | −0.101 |
| Vizeu | VIZ-01 | Vieira *et al.* (unpublished data) | Brazil | −1.88 | −46.75 | 10* | Terra firme | 2 | 30.37 | 328.6/334.37 | 4.05 | 2369 | 26.47 | 16.12 | −0.240 |
| Xingu: Arawete | XIN-01[1,2,3] | Balee & Campbell (1990) | Brazil | −4.82 | −52.52 | 35* | Terra firme | 1 | 22.10 | 240.05/224.35 | 4.41 | 2028 | 26.10 | 15.39 | −0.177 |
| Xingu: Asurini | XIN-02[1,2,3] | Balee & Campbell (1990) | Brazil | −4.75 | −52.6 | 35* | Terra firme | 1 | 21.90 | 237.93/222.33 | 4.41 | 2028 | 26.10 | 15.39 | −0.177 |
| Xingu: O Deserto 1 | XIN-03[1,2,3] | Campbell *et al.* (1986) | Brazil | −3.48 | −51.67 | 175* | Terra firme | 1 | 27.63 | 300.57/280.49 | 4.77 | 2085 | 26.59 | 15.31 | −0.181 |
| Xingu: O Deserto 2 | XIN-04 | Campbell *et al.* (1986) | Brazil | −3.48 | −51.67 | 175* | Terra firme | 1 | 32.14 | 349.63/326.27 | 4.77 | 2085 | 26.59 | 15.31 | −0.181 |
| Xingu: O Deserto 3 | XIN-05 | Campbell *et al.* (1986) | Brazil | −3.48 | −51.67 | 175* | Terra firme | 1 | 28.27 | 307.49/286.95 | 4.77 | 2085 | 26.59 | 15.31 | −0.181 |

Table A1. (Contd.)

| Plot Name | Plot Code | | Country | Latitude (decimal) | Longitude (decimal) | Elevation (m) | Forest Type | Plot Size (ha) | Basal area ($m^2 ha^{-1}$) | Biomass$^+$ (Mg DW $ha^{-1}$) | Mean number of months <100 mm of rainfall | Mean monthly rainfall (mm) | Mean monthly temperature (°C) | Mean monthly solar ($MJ m^{-2} day^{-1}$) | ENSO-rainfall correlation |
|---|---|---|---|---|---|---|---|---|---|---|---|---|---|---|---|
| Amacayacu: Lorena | AML-01 | Rudas, Prieto pers comm. | Colombia | −3.68 | −70.3 | 100* | Terra firme | 2 | 33.28 | 340.46/338.25 | 1.10 | 2619 | 25.83 | 15.31 | −0.154 |
| Anangu A1 | ANN-01 | Korning & Balslev (1994) | Ecuador | −0.53 | −76.43 | 250 | Seasonally flooded | 1.1 | 33.46 | 327.25/309.06 | 0.31 | 3252 | 25.97 | 15.23 | −0.158 |
| Anangu A2 | ANN-02 | Korning & Balslev (1994) | Ecuador | −0.53 | −76.43 | 310 | Terra firme | 1 | 33.82 | 330.82/312.44 | 0.31 | 3252 | 25.97 | 15.23 | −0.158 |
| Anangu A3 (Korning plot 2) | ANN-03 | Korning & Balslev (1994) | Ecuador | −0.53 | −76.43 | 370 | Terra firme | 1 | 24.00 | 234.76/221.72 | 0.31 | 3252 | 25.97 | 15.23 | −0.158 |
| Bogi 1 | BOG-01 | RAINFOR (unpublished data) | Ecuador | −0.7 | −76.48 | 270* | Terra firme | 1 | 30.78 | **299.61** | 0.31 | 3252 | 25.97 | 15.23 | −0.158 |
| Bogi 2 | BOG-02 | RAINFOR (unpublished data) | Ecuador | −0.7 | −76.47 | 270* | Terra firme | 1 | 26.00 | **232.88** | 0.31 | 3252 | 25.97 | 15.23 | −0.158 |
| Bogi 3 | BOG-03 | Pitman *et al.* (2001) | Ecuador | −0.69 | −76.47 | 270* | Terra firme | 1 | 28.70 | 280.61/265.61 | 0.31 | 3252 | 25.97 | 15.23 | −0.158 |
| Bogi 4 | BOG-04 | Pitman *et al.* (2001) | Ecuador | −0.7 | −76.47 | 270* | Terra firme | 1 | 37.30 | 364.71/345.2 | 0.31 | 3252 | 25.97 | 15.23 | −0.158 |
| Bogi 5 | BOG-05[1,2] | Pitman *et al.* (2001) | Ecuador | −0.7 | −76.48 | 270* | Terra firme | 1 | 18.90 | 184.74/174.91 | 0.31 | 3252 | 25.97 | 15.23 | −0.158 |
| Capiron | CAN-01 | Pitman *et al.* (2001) | Ecuador | −0.63 | −76.46 | 240* | Terra firme | 1 | 35.30 | 345.17/326.69 | 0.31 | 3252 | 25.97 | 15.23 | −0.158 |
| Jatun Sacha 2 | JAS-02[3] | RAINFOR (unpublished data) | Ecuador | −1.07 | −77.6 | 450 | Terra firme | 1 | 29.78 | **273.53** | 0.18 | 4013 | 23.31 | 15.19 | −0.013 |
| Jatun Sacha 3 | JAS-03 | RAINFOR (unpublished data) | Ecuador | −1.07 | −77.67 | 450 | Terra firme | 1 | 30.58 | **282.63** | 0.18 | 4013 | 23.31 | 15.19 | −0.013 |
| Jatun Sacha 4 | JAS-04 | RAINFOR (unpublished data) | Ecuador | −1.07 | −77.67 | 450 | Terra firme | 0.92 | 36.99 | **332.9** | 0.18 | 4013 | 23.31 | 15.19 | −0.013 |
| Jatun Sacha 5 | JAS-05 | RAINFOR (unpublished data) | Ecuador | −1.07 | −77.67 | 450 | Terra firme | 1 | 35.25 | **304.84** | 0.18 | 4013 | 23.31 | 15.19 | −0.013 |
| Payamino | PAY-01 | Pitman *et al.* (2001) | Ecuador | −0.45 | −76.03 | 275* | Terra firme | 1 | 29.60 | 290.72/288.58 | 0.26 | 3232 | 25.98 | 15.19 | −0.185 |
| Pirana | PIR-01 | Pitman *et al.* (2001) | Ecuador | −0.66 | −76.45 | 275* | Terra firme | 1 | 37.80 | 369.6/349.83 | 0.31 | 3252 | 25.97 | 15.23 | −0.158 |
| Shipati 1 | SHI-01 | Pitman *et al.* (2001) | Ecuador | −0.52 | −76.54 | 275* | Terra firme | 1 | 26.10 | 255.06/241.55 | 0.26 | 3482 | 25.78 | 15.17 | −0.132 |
| Shipati 2 | SHI-02 | Pitman *et al.* (2001) | Ecuador | −0.51 | −76.54 | 275* | Terra firme | 1 | 34.00 | 332.26/314.66 | 0.26 | 3482 | 25.78 | 15.17 | −0.132 |
| Shipati 3 | SHI-03 | Pitman *et al.* (2001) | Ecuador | −0.52 | −76.54 | 275* | Terra firme | 1 | 38.50 | 376.23/356.31 | 0.26 | 3482 | 25.78 | 15.17 | −0.132 |
| Shiripuno | SHR-01 | Pitman *et al.* (2001) | Ecuador | −1.02 | −76.98 | 300* | Terra firme | 1 | 22.90 | 223.53/211.93 | 0.13 | 3498 | 25.69 | 15.24 | −0.087 |
| Tiputini 2 | TIP-02 | RAINFOR (unpublished data) | Ecuador | −0.63 | −76.14 | 275* | Terra firme | 0.8 | 27.98 | **273.24** | 0.31 | 3252 | 25.97 | 15.23 | −0.158 |
| Tiputini 3 | TIP-03 | RAINFOR (unpublished data) | Ecuador | −0.64 | −76.15 | 275* | Seasonally flooded | 1 | 24.17 | **260.54** | 0.31 | 3252 | 25.97 | 15.23 | −0.158 |
| Saint Elie Transect 1 (0.78 ha) | ELI-01 | Chave (2001) | French Guiana | 5.5 | −53 | 25* | Terra firme | 0.78 | 35.56 | 385.83/361.65 | 3.28 | 3000 | 26.32 | 18.15 | −0.178 |

Table A1. (Contd.)

| Plot Name | Plot Code | | Country | Latitude (decimal) | Longitude (decimal) | Elevation (m) | Forest Type | Plot Size (ha) | Basal area ($m^2\,ha^{-1}$) | Biomass$^+$ (Mg DW $ha^{-1}$) | Mean number of months <100 mm of rainfall | Mean monthly rainfall (mm) | Mean monthly temperature (°C) | Mean monthly solar ($MJ\,m^{-2}\,day^{-1}$) | ENSO-rainfall correlation |
|---|---|---|---|---|---|---|---|---|---|---|---|---|---|---|---|
| Saint Elie Transect 2 (1 ha) | ELI-02 | Chave (2001) | French Guiana | 5.5 | −53 | 25* | Terra firme | 1 | 38.57 | 418.48/392.26 | 3.28 | 3000 | 26.32 | 18.15 | −0.178 |
| Nouragues PP | NOR-01 | Chave (2001) | French Guiana | 4.08 | −52.67 | 110 | Terra firme | 12 | 31.00 | 336.23/319.3 | 2.59 | 3155 | 25.34 | 17.60 | −0.231 |
| Nouragues GP | NOR-02 | Chave (2001) | French Guiana | 4.08 | −52.67 | 110 | Terra firme | 10 | 28.23 | 306.18/290.77 | 2.59 | 3155 | 25.34 | 17.60 | −0.231 |
| Paracou | PAR | Gourlet-Fleury & Houllier (2000) | French Guiana | 5.25 | −52.83 | 25* | Terra firme | 6.25 | 30.77 | 334.34/326.58 | 3.28 | 3000 | 26.32 | 18.15 | −0.178 |
| Berbice River Kwakwani 1 | BER-01 | Comiskey *et al.* (1994) | Guyana | 5.5 | −58 | 50* | Terra firme | 1 | 23.68 | 255.54/255.7 | 2.85 | 2505 | 26.78 | 17.57 | −0.193 |
| Berbice River Kwakwani 2 | BER-02 | Comiskey *et al.* (1994) | Guyana | 5.5 | −58 | 50* | Terra firme | 1 | 27.56 | 297.41/297.6 | 2.85 | 2505 | 26.78 | 17.57 | −0.193 |
| Kurupukari: Mora | KUR-01 | Johnston & Gillman (1995) | Guyana | 4.58 | −58.72 | 120* | Terra firme | 1 | 24.33 | 263.22/262.72 | 2.26 | 3052 | 26.10 | 17.73 | −0.188 |
| Kurupukari: TA2 | KUR-02 | Johnston & Gillman (1995) | Guyana | 4.58 | −58.72 | 120* | Terra firme | 1 | 28.43 | 307.57/307 | 2.26 | 3052 | 26.10 | 17.73 | −0.188 |
| Kurupukari: TA12 | KUR-03 | Johnston & Gillman (1995) | Guyana | 4.58 | −58.72 | 120* | Terra firme | 1 | 26.55 | 287.23/286.69 | 2.26 | 3052 | 26.10 | 17.73 | −0.188 |
| Kurupukari: TA19 | KUR-04 | Johnston & Gillman (1995) | Guyana | 4.58 | −58.72 | 120* | Terra firme | 1 | 26.55 | 287.23/286.69 | 2.26 | 3052 | 26.10 | 17.73 | −0.188 |
| North West District: Kariako | NWD-01 | van Andel (2001) | Guyana | 7.42 | −59.73 | 30* | Terra firme | 1 | 32.91 | 352.56/339.63 | 1.97 | 2555 | 25.72 | 17.32 | −0.191 |
| North West District: Santa Rosa | NWD-02 | van Andel (2001) | Guyana | 7.6 | −58.95 | 30* | Terra firme | 1 | 34.55 | 370.6/356.56 | 2.67 | 2379 | 26.34 | 17.95 | −0.179 |
| BCI 50 ha | BCI-50 | | Panama | 9.17 | −79.85 | 30* | n/n | 50 | 28.56 | 290.22/294.17 | 3.54 | 2912 | 25.96 | 17.91 | −0.057 |
| Allpahuayo C | ALP-30 | RAINFOR (unpublished data) | Peru | −3.95 | −73.42 | 120* | Terra firme | 1 | 23.13 | 232.44/239.47 | 0.77 | 2763 | 26.46 | 15.69 | −0.028 |
| Amigos downriver 1 | AMD-01 | Pitman *et al.* (2001) | Peru | −12.53 | −70.08 | 230* | Terra firme | 1 | 25.80 | 261.08/261.66 | 0.77 | 4027 | 24.26 | 18.08 | −0.043 |
| Amigos downriver 2 | AMD-02 | Pitman *et al.* (2001) | Peru | −12.53 | −70.08 | 230* | Terra firme | 1 | 22.90 | 231.73/232.25 | 0.77 | 4027 | 24.26 | 18.08 | −0.043 |
| Amigos upriver 1 | AMU-01 | Pitman *et al.* (2001) | Peru | −12.5 | −70.1 | 230* | Terra firme | 1 | 27.90 | 282.3/282.96 | 0.77 | 4027 | 24.26 | 18.08 | −0.043 |
| Amigos upriver 2 | AMU-02 | Pitman *et al.* (2001) | Peru | −12.5 | −70.1 | 230* | Terra firme | 1 | 25.30 | 255.99/256.59 | 0.77 | 4027 | 24.26 | 18.08 | −0.043 |
| Barranco | BAC-01 | Pitman *et al.* (2001) | Peru | −11.88 | −71.38 | 400* | Terra firme | 0.88 | 32.05 | 323.31/325.05 | 1.59 | 3043 | 24.56 | 17.44 | −0.121 |

Table A1. (Contd.)

| Plot Name | Plot Code | | Country | Latitude (decimal) | Longitude (decimal) | Elevation (m) | Forest Type | Plot Size (ha) | Basal area ($m^2\,ha^{-1}$) | Biomass[+] (Mg DW $ha^{-1}$) | Mean number of months <100 mm of rainfall | Mean monthly rainfall (mm) | Mean monthly temperature (°C) | Mean monthly solar ($MJ\,m^{-2}\,day^{-1}$) | ENSO-rainfall correlation |
|---|---|---|---|---|---|---|---|---|---|---|---|---|---|---|---|
| Cabeza de Mono | CAB-01 | Gentry & Smith (unpublished data) | Peru | −10.33 | −75.3 | 340 | Terra firme | 1 | 29.11 | 290.23/295.18 | 3.38 | 2244 | 22.39 | 16.33 | −0.063 |
| Camisea: San Martin-3.1 | CAM-01[1] | Comiskey *et al*. (2001) | Peru | −11.78 | −72.7 | 487 | Terra firme | 1 | 22.16 | 223.37/225.03 | 3.08 | 2287 | 23.66 | 17.25 | −0.116 |
| Camisea: San Martin-3.2 | CAM-02[1,2,3] | Comiskey *et al*. (2001) | Peru | −11.78 | −72.7 | 487 | Terra firme | 1 | 19.06 | 192.12/193.55 | 3.08 | 2287 | 23.66 | 17.25 | −0.116 |
| Camisea: Cashiriari 2 | CAM-03 | Comiskey *et al*. (2001) | Peru | −11.86 | −72.77 | 469 | Terra firme | 1 | 34.94 | 352.21/354.81 | 3.08 | 2287 | 23.66 | 17.25 | −0.116 |
| Camisea: Pagoreni | CAM-04 | Comiskey *et al*. (2001) | Peru | −11.78 | −72.7 | 465 | Terra firme | 1 | 27.77 | 279.92/282 | 3.08 | 2287 | 23.66 | 17.25 | −0.116 |
| Camisea: Las Malvinas | CAM-05 | Comiskey *et al*. (2001) | Peru | −11.88 | −72.93 | 480 | Terra firme | 1 | 30.20 | 303.12/306.68 | 3.08 | 2287 | 23.66 | 17.25 | −0.116 |
| Camisea: Segakiato-1 | CAM-06 | Comiskey *et al*. (2001) | Peru | −11.79 | −72.87 | 450 | Terra firme | 1 | 28.04 | 281.44/284.74 | 3.08 | 2287 | 23.66 | 17.25 | −0.116 |
| Camisea: Segakiato-2 | CAM-07 | Comiskey *et al*. (2001) | Peru | −11.8 | −72.92 | 400 | Terra firme | 1 | 30.26 | 303.52/307.29 | 3.08 | 2287 | 23.66 | 17.25 | −0.116 |
| Camisea: Shivankoreni-2 | CAM-08 | Comiskey *et al*. (2001) | Peru | −11.69 | −72.97 | 350 | Terra firme | 1 | 27.51 | 275.88/279 | 3.08 | 2287 | 23.66 | 17.25 | −0.116 |
| Camisea: Shivankoreni-1 | CAM-09 | Comiskey *et al*. (2001) | Peru | −11.79 | −72.92 | 400 | Terra firme | 1 | 33.96 | 340.63/344.86 | 3.08 | 2287 | 23.66 | 17.25 | −0.116 |
| Camisea: Peruanita | CAM-10[1,2,3] | Comiskey *et al*. (2001) | Peru | −11.67 | −72.99 | 350 | Terra firme | 1 | 21.40 | 214.59/217.04 | 3.08 | 2287 | 23.66 | 17.25 | −0.116 |
| Camisea: Cashiriari 3 | CAM-11 | Comiskey *et al*. (2001) | Peru | −11.86 | −72.77 | 579 | Terra firme | 1 | 28.58 | 288.1/290.23 | 3.08 | 2287 | 23.66 | 17.25 | −0.116 |
| Cuzco Amazonico CUZAM1E | CUZ-01 | RAINFOR (unpublished data) | Peru | −12.5 | −68.95 | 200* | Terra firme | 1 | 28.24 | **296.4** | 4.15 | 2106 | 25.37 | 17.92 | 0.050 |
| Cuzco Amazonico CUZAM1U | CUZ-02 | RAINFOR (unpublished data) | Peru | −12.5 | −68.95 | 200* | Terra firme | 1 | 28.15 | **272.58** | 4.15 | 2106 | 25.37 | 17.92 | 0.050 |
| Cuzco Amazonico CUZAM2E | CUZ-03 | RAINFOR (unpublished data) | Peru | −12.49 | −69.11 | 200* | Terra firme | 1 | 25.19 | **268.48** | 3.90 | 2162 | 25.09 | 17.82 | 0.034 |
| Cuzco Amazonico CUZAM2U | CUZ-04 | RAINFOR (unpublished data) | Peru | −12.49 | −69.11 | 200* | Terra firme | 1 | 29.29 | **308.51** | 3.90 | 2162 | 25.09 | 17.82 | 0.034 |
| Indiana | IND-01 | RAINFOR (unpublished data) | Peru | −3.52 | −72.85 | 100* | Terra firme | 1 | 31.97 | 321.94/311.71 | 0.74 | 2623 | 26.43 | 15.63 | −0.027 |
| Jenaro High Restinga Plot 1 | JEN-01 | Nebel (2001) | Peru | −4.92 | −73.73 | 100* | Seasonally flooded | 1 | 25.07 | 248.25/244.42 | 0.97 | 2452 | 26.81 | 15.41 | −0.032 |

 

Table A1. (Contd.)

| Plot Name | Plot Code | | Country | Latitude (decimal) | Longitude (decimal) | Elevation (m) | Forest Type | Plot Size (ha) | Basal area ($m^2 ha^{-1}$) | Biomass$^+$ (Mg DW $ha^{-1}$) | Mean number of months <100 mm of rainfall | Mean monthly rainfall (mm) | Mean monthly temperature (°C) | Mean monthly solar ($MJ m^{-2} day^{-1}$) | ENSO-rainfall correlation |
|---|---|---|---|---|---|---|---|---|---|---|---|---|---|---|---|
| Jenaro High Restinga Plot 2 | JEN-02 | Nebel (2001) | Peru | −4.92 | −73.73 | 100* | Seasonally flooded | 1 | 25.03 | 247.85/244.03 | 0.97 | 2452 | 26.81 | 15.41 | −0.032 |
| Jenaro High Restinga Plot 3 | JEN-03 | Nebel (2001) | Peru | −4.92 | −73.73 | 100* | Seasonally flooded | 1 | 26.02 | 257.65/253.68 | 0.97 | 2452 | 26.81 | 15.41 | −0.032 |
| Jenaro Low Restinga Plot 4 | JEN-04[1,2,3] | Nebel (2001) | Peru | −4.92 | −73.73 | 100* | Seasonally flooded | 1 | 19.88 | 196.85/193.82 | 0.97 | 2452 | 26.81 | 15.41 | −0.032 |
| Jenaro Low Restinga plot 5 | JEN-05 | Nebel (2001) | Peru | −4.92 | −73.73 | 100* | Seasonally flooded | 1 | 23.67 | 234.38/230.77 | 0.97 | 2452 | 26.81 | 15.41 | −0.032 |
| Jenaro Low Restinga plot 6 | JEN-06 | Nebel (2001) | Peru | −4.92 | −73.73 | 100* | Seasonally flooded | 1 | 27.20 | 269.34/265.18 | 0.97 | 2452 | 26.81 | 15.41 | −0.032 |
| Jenaro Tahuampa Plot 7 | JEN-07 | Nebel (2001) | Peru | −4.92 | −73.73 | 100* | Seasonally flooded | 1 | 27.14 | 268.74/264.6 | 0.97 | 2452 | 26.81 | 15.41 | −0.032 |
| Jenaro Tahuampa Plot 8 | JEN-08 | Nebel (2001) | Peru | −4.92 | −73.73 | 100* | Seasonally flooded | 1 | 28.84 | 285.58/281.17 | 0.97 | 2452 | 26.81 | 15.41 | −0.032 |
| Jenaro Tahuampa Plot 9 | JEN-09 | Nebel (2001) | Peru | −4.92 | −73.73 | 100* | Seasonally flooded | 1 | 28.24 | 279.64/275.32 | 0.97 | 2452 | 26.81 | 15.41 | −0.032 |
| Jenaro Herrera: Spichiger | JEN-10 | Spichiger *et al.* (1996) | Peru | −4.92 | −73.73 | 100* | Terra firme | 1 | 23.60 | 233.69/230.09 | 0.97 | 2452 | 26.81 | 15.41 | −0.032 |
| Maizal 1 | MAI-01 | Pitman *et al.* (2001) | Peru | −11.8 | −71.47 | 400* | Terra firme | 1 | 30.10 | 303.59/302.95 | 1.59 | 3043 | 24.56 | 17.44 | −0.121 |
| Maizal 2 | MAI-02 | Pitman *et al.* (2001) | Peru | −11.8 | −71.47 | 400* | Terra firme | 1 | 32.60 | 328.8/328.1 | 1.59 | 3043 | 24.56 | 17.44 | −0.121 |
| Manu alluvial Cocha Cashu Trail 3 M1 | MNU-01 | Pitman *et al.* (2001) | Peru | −11.88 | −71.35 | 400 | Rarely flooded | 0.97 | 29.54 | 298/299.59 | 1.59 | 3043 | 24.56 | 17.44 | −0.121 |
| Manu terra firme terrace M3 | MNU-03 | Terborgh *et al.* (unpublished data) | Peru | −11.88 | −71.35 | 400 | Terra firme | 2 | 26.41 | 266.42/267.85 | 1.59 | 3043 | 24.56 | 17.44 | −0.121 |
| Manu terra firme ravine M4 | MNU-04 | Terborgh *et al.* (unpublished data) | Peru | −11.88 | −71.35 | 400 | Terra firme | 2 | 28.46 | 287.1/288.64 | 1.59 | 3043 | 24.56 | 17.44 | −0.121 |
| Manu alluvial Cocha Cashu Trail 12 | MNU-05 | Terborgh *et al.* (unpublished data) | Peru | −11.88 | −71.35 | 400 | Rarely flooded | 2 | 34.64 | 349.44/351.32 | 1.59 | 3043 | 24.56 | 17.44 | −0.121 |
| Manu alluvial Cocha Cashu Trail 2 & 31 | MNU-06 | Terborgh *et al.* (unpublished data) | Peru | −11.88 | −71.35 | 400 | Rarely flooded | 2.25 | 33.84 | 341.37/343.2 | 1.59 | 3043 | 24.56 | 17.44 | −0.121 |
| Cocha Salvador Manu mature floodplain | MNU-08[1,2] | Terborgh *et al.* (unpublished data) | Peru | −11.88 | −71.3 | 400 | Rarely flooded | 2 | 38.01 | 383.45/382.56 | 1.59 | 3043 | 24.56 | 17.44 | −0.121 |

Table A1. (Contd.)

| Plot Name | Plot Code | | Country | Latitude (decimal) | Longitude (decimal) | Elevation (m) | Forest Type | Plot Size (ha) | Basal area ($m^2\,ha^{-1}$) | Biomass$^+$ (Mg DW $ha^{-1}$) | Mean number of months <100 mm of rainfall | Mean monthly rainfall (mm) | Mean monthly temperature (°C) | Mean monthly solar ($MJ\,m^{-2}\,day^{-1}$) | ENSO-rainfall correlation |
|---|---|---|---|---|---|---|---|---|---|---|---|---|---|---|---|
| Mishana | MSH-01[3] | RAINFOR (unpublished data) | Peru | −3.78 | −73.5 | 120* | Terra firme | 1 | 29.43 | 295.91/304.69 | 0.77 | 2763 | 26.46 | 15.69 | −0.028 |
| Pakitza Manu River dissected alluvial plot 1 | PAK-01 | RAINFOR (unpublished data) | Peru | −11.93 | −71.25 | 400* | n/n | 1 | 25.98 | 262.11/263.49 | 1.59 | 3043 | 24.56 | 17.44 | −0.121 |
| Pakitza Manu River alluvial plot 2 | PAK-02[1,2,3] | RAINFOR (unpublished data) | Peru | −11.93 | −71.25 | 400* | n/n | 1 | 37.20 | 375.31/377.28 | 1.59 | 3043 | 24.56 | 17.44 | −0.121 |
| Pakitza Manu river swamp | PAK-03 | RAINFOR (unpublished data) | Peru | −11.93 | −71.25 | 400* | n/n | 1 | 29.98 | 302.47/304.05 | 1.59 | 3043 | 24.56 | 17.44 | −0.121 |
| Pakitza Manu river swamp | PAK-04 | RAINFOR (unpublished data) | Peru | −11.93 | −71.25 | 400* | n/n | 1 | 30.02 | 302.87/304.46 | 1.59 | 3043 | 24.56 | 17.44 | −0.121 |
| Rio Piedras | RPI-01[3] | Terborgh *et al.* (unpublished data) | Peru | −12.35 | −69.23 | 200* | Terra firme | 1 | 25.30 | 255.5/249.85 | 3.90 | 2162 | 25.09 | 17.82 | 0.034 |
| Sucusari A | SUC-01 | RAINFOR (unpublished data) | Peru | −3.23 | −72.9 | 100* | Terra firme | 1 | 27.89 | **289.03** | 0.54 | 2671 | 26.37 | 15.63 | −0.025 |
| Sucusari B | SUC-02 | RAINFOR (unpublished data) | Peru | −3.23 | −72.9 | 100* | Terra firme | 1 | 27.76 | **294.46** | 0.54 | 2671 | 26.37 | 15.63 | −0.025 |
| Sucusari C | SUC-03 | RAINFOR (unpublished data) | Peru | −3.25 | −72.93 | 100* | Seasonally flooded | 1 | 26.38 | **315.9** | 0.54 | 2671 | 26.37 | 15.63 | −0.025 |
| Sucusari D | SUC-04 | RAINFOR (unpublished data) | Peru | −3.25 | −72.89 | 100* | Terra firme | 1 | 29.62 | **307.04** | 0.54 | 2671 | 26.37 | 15.63 | −0.025 |
| Sucusari E | SUC-05 | RAINFOR (unpublished data) | Peru | −3.26 | −72.9 | 100* | Terra firme | 1 | 27.70 | **297.78** | 0.54 | 2671 | 26.37 | 15.63 | −0.025 |
| Tambopata plot zero | TAM-01 | RAINFOR (unpublished data) | Peru | −12.85 | −69.28 | 230* | Terra firme | 1 | 28.86 | **294.83** | 3.46 | 2417 | 25.09 | 17.99 | 0.048 |
| Tambopata plot one | TAM-02 | RAINFOR (unpublished data) | Peru | −12.83 | −69.28 | 230* | Terra firme | 1 | 29.96 | **289.75** | 3.46 | 2417 | 25.09 | 17.99 | 0.048 |
| Tambopata plot three | TAM-05 | RAINFOR (unpublished data) | Peru | −12.83 | −69.28 | 230* | Terra firme | 1 | 26.56 | **294.12** | 3.46 | 2417 | 25.09 | 17.99 | 0.048 |
| Tambopata plot four | TAM-06[1,2] | RAINFOR (unpublished data) | Peru | −12.83 | −69.3 | 230* | Terra firme† | 0.96 | 36.05 | **266.91** | 3.46 | 2417 | 25.09 | 17.99 | 0.048 |
| Tambopata plot six | TAM-07 | RAINFOR (unpublished data) | Peru | −12.83 | −69.27 | 230* | Terra firme | 1 | 28.95 | **325.74** | 3.46 | 2417 | 25.09 | 17.99 | 0.048 |
| Tambopata Ccolpa pacal upland | TCP-02 | Terborgh *et al.* (unpublished data) | Peru | −13.13 | −69.56 | 420* | Terra firme | 2.25 | 24.12 | **255.95** | 1.36 | 3673 | 23.58 | 18.29 | 0.026 |

Table A1. (Contd.)

| Plot Name | Plot Code | | Country | Latitude (decimal) | Longitude (decimal) | Elevation (m) | Forest Type | Plot Size (ha) | Basal area ($m^2\,ha^{-1}$) | Biomass[+] (Mg DW $ha^{-1}$) | Mean number of months <100 mm of rainfall | Mean monthly rainfall (mm) | Mean monthly temperature (°C) | Mean monthly solar (MJ $m^{-2}$ $day^{-1}$) | ENSO-rainfall correlation |
|---|---|---|---|---|---|---|---|---|---|---|---|---|---|---|---|
| Yanamono A | YAN-01[1,3] | RAINFOR (unpublished data) | Peru | −3.43 | −72.85 | 100* | Terra firme | 1 | 32.41 | **317.78** | 0.54 | 2671 | 26.37 | 15.63 | −0.025 |
| Yanamono B | YAN-02 | RAINFOR (unpublished data) | Peru | −3.43 | −72.84 | 100* | Terra firme | 1 | 30.60 | **319.24** | 0.54 | 2671 | 26.37 | 15.63 | −0.025 |
| El Caura | CAU-01 | Castellanos (1998) | Venezuela | −6.36 | −64.99 | 65* | Terra firme | 13 | 34.46 | 365.31/335.96 | 3.08 | 2283 | 26.51 | 15.29 | −0.087 |
| Cano Rosalba Z1 CR1 (upland) | CRS-01 | Veillon (1985) | Venezuela | 9.25 | −72 | 60 | Terra firme | 1 | 18.19 | 186.27/188.63 | 6.00 | 1324 | 28.23 | 17.33 | −0.227 |
| Cano Rosalba Z2 CR2 (alluvial) | CRS-02 | Veillon (1985) | Venezuela | 9.25 | −72 | 35 | Terra firme | 1 | 29.59 | 303/306.85 | 6.00 | 1324 | 28.23 | 17.33 | −0.227 |
| Cerro Neblina | NEB-01 | Gentry (unpublished data) | Venezuela | 0.83 | −66.17 | 600* | Terra firme | 1 | 27.92 | 302.09/306.56 | 0.51 | 2856 | 24.94 | 16.48 | −0.177 |
| San Carlos de Rio Negro SC1 Uhl | SCR-01 | Uhl *et al*. (1988) | Venezuela | 1.93 | −67.05 | 119 | Terra firme | 1 | 27.80 | 300.63/273.66 | 0.33 | 3178 | 26.02 | 16.62 | −0.109 |
| San Carlos de Rio Negro SC3 MAB site | SCR-03 | Veillon, Brown, Phillips, Lewis (unpublished data) | Venezuela | 1.75 | −67 | 100* | Terra firme | 2 | 33.02 | 357.08/325.05 | 0.46 | 3093 | 26.23 | 16.75 | −0.113 |

For biomass, values in bold represent direct individual-tree based biomass estimates taken from Baker *et al*. (2004). The remaining estimates are calculated using the interpolated structural conversion factor as detailed in the text, with the first value based on the kriged interpolation, the second value based on the soils-based interpolation. Superscripts next to the biomass value indicate plots with outlying values of biomass, that were removed from analysis as follows:

[1]Anomalous plots removed from the interpolation of basal area using the optimum plot removal procedure as described in the text.

[2]Anomalous plots removed from the kriged interpolation of plot biomass values using the optimum plot removal procedure as described in the text.

[3]Anomalous plots removed from the soils-based interpolation of plot biomass values using the optimum plot removal procedure as described in the text.

*For elevation values were derived from a 1 km resolution digital elevation model.

†For forest descriptions, a plot with <0.2 ha of rarely flooded forest.